SYNTHESIS AND REACTIVITY OF ALKENYL AND ALKYNYL DERIVATIVES OF PERMETHYLZIRCONOCENE AND PERMETHYLHAFNOCENE. REARRANGEMENT OF ALKENYL DERIVATIVES INVOLVING β-H ELIMINATION FROM AN sp²-HYBRIDIZED CARBON *·**

CHRISTINE McDADE *** and JOHN E. BERCAW*

Arthur Amos Noyes Laboratory of Chemical Physics [†], California Institute of Technology, Pasadena, California 91125 (U.S.A.)

(Received April 6th, 1984)

Summary

The insertion of unactivated acetylenes into the metal–hydride bonds of (η^5-C$_5$Me$_5$)$_2$MH$_2$ (M = Zr, Hf) proceeds rapidly at low temperature to form mono- and/or bisinsertion products, dependent on the steric bulk of the acetylene substituents. 2-Butyne and t-butylacetylene react to form (η^5-C$_5$Me$_5$)$_2$M(H)-(C(Me)=CHMe) and (η^5-C$_5$Me$_5$)$_2$M(H)(CH=CHCMe$_3$) (M = Zr, Hf). Propyne and 1-butyne react to form (η^5-C$_5$Me$_5$)$_2$M(CH=CHCH$_3$)$_2$ (M = Zr, Hf) and (η^5-C$_5$Me$_5$)$_2$Zr(CH=CHCH$_2$CH$_3$)$_2$. Phenylacetylene yields both (η^5-C$_5$Me$_5$)$_2$M(H)(CH=CHPh) and (η^5-C$_5$Me$_5$)$_2$M(CH=CHPh)$_2$ (M = Zr, Hf). To extend the study of the unsaturated carbon ligands, the bis(propynyl) complexes (η^5-C$_5$Me$_5$)$_2$M(C≡CCH$_3$)$_2$ (M = Zr, Hf) are prepared by treating (η^5-C$_5$Me$_5$)$_2$MCl$_2$ with LiC≡CCH$_3$. The reactivity of many of these complexes with carbon monoxide and dihydrogen is surveyed.

The mono(2-butenyl)zirconium complex (η^5-C$_5$Me$_5$)$_2$Zr(H)(C(Me)=CHMe) rearranges, forming the crotyl-hydride species (η^5-C$_5$Me$_5$)$_2$Zr(H)(η^3-C$_4$H$_7$) or, in the presence of 2-butyne, the zirconacyclopentene (η^5-C$_5$Me$_5$)$_2$-ZrCH$_2$CH(CH$_2$CH$_3$)C(CH$_3$)=C(CH$_3$). The hafnium analog (η^5-C$_5$Me$_5$)$_2$Hf-

---

(H)(C(Me)=CHMe) also rearranges, although more slowly and less cleanly, to the analogous crotyl-hydride hafnium species. The bis(propenyl) and bis(butenyl)zirconium complexes also rearrange, forming zirconacyclopentenes (η^5-$C_5Me_5)_2ZrCH_2CH(R)CH=CR$ and (η^5-$C_5Me_5)_2ZrCH_2CH(R)C(R)=CH$ (R = CH_3, CH_2CH_3). The bis(propenyl)hafnium complex is stable to rearrangement. Mechanistic and kinetic studies of these transformations demonstrate the occurrence of an unusual β-hydrogen elimination from an sp^2-hybridized carbon.

Introduction

The reactions of unsaturated hydrocarbons with transition metal compounds are of fundamental importance in organometallic chemistry [1]. Insertion of olefins and acetylenes into metal–hydrogen and metal–carbon bonds are requisite steps in industrially important processes such as isomerization, hydrogenation, and polymerization as well as in stoichiometric transformations for organic synthesis. Whereas the reactions of late transition metal hydrides with acetylenes have been extensively documented [2,3], less is known concerning the reactions of early transition metal hydrides with acetylenes or the chemistry available to the resultant alkenyl insertion products.

Labinger and Schwartz have described the *cis* addition of Zr–H to terminal and internal acetylenes, and together with Negishi, have documented its synthetic utility [4,5]. Wailes et al. [6] briefly reported on the reactions of $[(\eta^5\text{-}C_5H_5)_2ZrHCl]_x$ and $[(\eta^5\text{-}C_5H_5)_2ZrH_2]_x$ with acetylenes; however, some of the products obtained, including the bis(alkenyl) derivatives, were not completely characterized. Bis(alkynyl) derivatives of zirconocene have also been described only briefly [7]. Most recently Erker and co-workers have systematically studied the alkenyl derivatives of $[(\eta^5\text{-}C_5H_5)_2ZrCl]$ and have reported some binuclear compounds with an unusual bridging alkenyl ligand [8].

During the course of our work with bis(pentamethylcyclopentadienyl) derivatives of zirconium and hafnium we noted that $Cp_2^\star MH_2$ ($Cp^\star \equiv \eta^5\text{-}C_5Me_5$; M = Zr, Hf) react with terminal olefins to afford very stable, monomeric, alkyl hydride derivatives [9]. Preliminary evidence showed that the alkenyl derivatives are even more robust; $Cp_2^\star Hf(H)(CH=CHCMe_3)$, obtained from $Cp_2^\star HfH_2$ and $HC\equiv CCMe_3$, is stable for days at 125°C [10]. We report herein our studies of alkenyl hydride and bis(alkenyl) derivatives of permethylzirconocene and permethylhafnocene obtained via insertion of unactivated acetylenes into metal–hydrogen bonds.
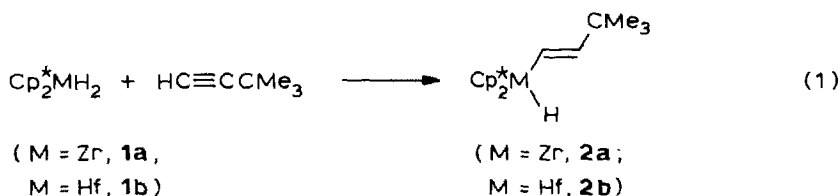
While the hafnium derivatives do prove relatively thermally stable, the zirconium analogs rearrange under mild conditions. The 2-butenyl hydride derivatives isomerize to a η^3-crotyl hydride species. The bis(alkenyl) derivatives rearrange to afford zirconacyclopentenes. The mechanisms of these transformations are explored and the latter transformation is shown to involve a rare example of β-hydrogen elimination from an sp^2-hybridized carbon [11].

To further extend this study of unsaturated carbon ligands, the reactivity of these compounds with carbon monoxide and dihydrogen is examined. Additionally, the bis(propynyl) derivatives of permethylzirconocene and permethylhafnocene are synthesized and the extent of their reactivity is explored.
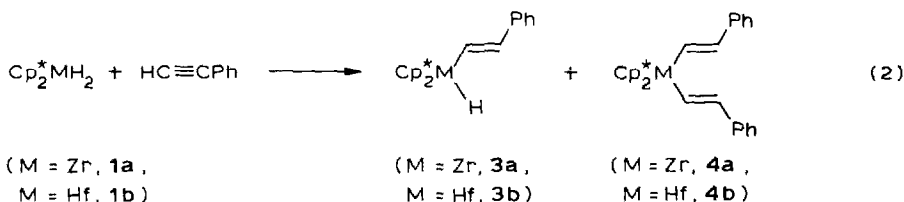
Results

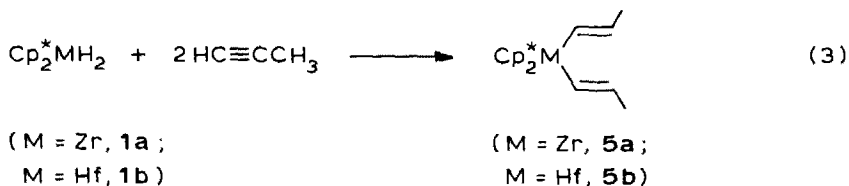*Synthesis and characterization of alkenyl derivatives of permethylzirconocene and permethylhafnocene*

The reactions of $Cp_2^*MH_2$ (M = Zr (**1a**) [9c], Hf (**1b**) [12]) with unactivated alkynes occur rapidly at room temperature in toluene, benzene, or petroleum ether solutions. The course of these reactions is highly dependent on the nature of the alkyne substituent(s). t-Butylacetylene adds to an M–H bond of $Cp_2^*MH_2$ (**1a** and **1b**) in a *cis* manner to afford the monoinsertion products $Cp_2^*M(H)(CH=CHCMe_3)$ (**2a** and **2b**) (eq. 1), isolable as colorless, crystalline solids [13]. The *trans* configura-

$$Cp_2^*MH_2 \ + \ HC\equiv CCMe_3 \longrightarrow \ Cp_2^*M \diagdown{}^{CMe_3}_{H} \qquad (1)$$

(M = Zr, **1a**,   (M = Zr, **2a**;
  M = Hf, **1b**)   M = Hf, **2b**)

tion about the double bond is supported by the large value of $^3J(HH)$ for the vinylic protons (21 Hz for **2a** and **2b**) (Table 1). On the other hand, the reactions of **1a** and **1b** with the less sterically demanding phenylacetylene yield mixtures of the mono- and bisinsertion products, $Cp_2^*M(H)(CH=CHPh)$ (**3a** and **3b**) and Cp_2^*M-$(CH=CHPh)_2$ (**4a** and **4b**) (eq. 2). These have been characterized by NMR spectros-

$$Cp_2^*MH_2 \ + \ HC\equiv CPh \longrightarrow \ Cp_2^*M\diagdown{}^{Ph}_{H} \ + \ Cp_2^*M\diagdown{}^{Ph}_{Ph} \qquad (2)$$

(M = Zr, **1a**,   (M = Zr, **3a**,   (M = Zr, **4a**,
  M = Hf, **1b**)   M = Hf, **3b**)   M = Hf, **4b**)

copy only, and also show large coupling of the vinylic protons ($^3J(HH)$ 20 Hz) [14]. With an even smaller substituent, methyl, on the acetylene, **1a** and **1b** react to form only the bisinsertion products $Cp_2^*M(CH=CHCH_3)_2$ (**5a** and **5b**) (eq. 3). As before,

$$Cp_2^*MH_2 \ + \ 2\,HC\equiv CCH_3 \longrightarrow \ Cp_2^*M \qquad (3)$$

(M = Zr, **1a**;   (M = Zr, **5a**;
  M = Hf, **1b**)   M = Hf, **5b**)

exclusively *cis* addition of the metal–hydride bond to the alkyne is observed, as judged by the magnitude of the vinylic H–H coupling ($^3J(HH)$ 18 Hz for **5a** and **5b**) (Table 1).

Compound **5a** forms very rapidly – the monoinsertion product is not observed, even by low temperature NMR spectrometry – and is isolated as an off-white microcrystalline solid in good yield (66%) from $-78°C$ petroleum ether solutions.

TABLE 1

NMR[a] AND IR[b] DATA

Compound	IR	NMR (Chemical shift, multiplicity (coupling constants))		
		Assignment	^{1}H	^{13}C
$Cp_2^*Zr(H)(CH=CHCMe_3)$ (**2a**)[c]		$C_5(CH_3)_5$	1.85 s	12.0 q (126)
		$ZrCH=CHC(CH_3)_3$	4.28 dd (21, 2.2)	116.5 s
		$ZrCH=CHC(CH_3)_3$	6.60 dd (21, 1.5)	191.9 dd (117, 10)
		$ZrCH=CHC(CH_3)_3$	1.17 s	140.1 d (146)
		$Zr-H$	5.73 s. br	30.1 q (122)
				38.1 s
$Cp_2^*Hf(H)(CH=CHCMe_3)$ (**2b**)[d]	ν(C=C) 1560	$C_5(CH_3)_5$	1.91 s	
	ν(Hf–H) 1625	$C_5(CH_3)_5$		
		$Hf[CH=CHC(CH_3)_3$	5.80 d (21)	
		$Hf[CH=CHC(CH_3)_3$	4.81 d (21)	
		$Hf[CH=CHC(CH_3)_3$	1.09 s	
		$Hf[CH=CHC(CH_3)_3$		
		$Hf-H$	12.83 s. br	
$Cp_2^*Zr(CH=CHCH_3)_2$ (**5a**)[e,f]	ν(C=C) 1570	$C_5(CH_3)_5$	1.76 s	11.8 q (125)
		$C_5(CH_3)_5$		117.9 s
		$ZrCH=CHCH_3$	5.83 dq (18, 1.5)	191.5 dq (114, 6)
		$ZrCH=CHCH_3$	5.21 dq (18, 5.5)	130.4 dq (148, 8)
		$ZrCH=CHCH_3$	1.90 dd (5.5, 1.5)	25.3 qdd (124, 12, 8)
$Cp_2^*Hf(CH=CHCH_3)_2$ (**5b**)[f]	ν(C=C) 1571	$C_5(CH_3)_5$	1.79 s	
		$Hf[CH=CHCH_3$	5.56 dq (18, 1.5)	
		$Hf[CH=CHCH_3$	5.24 dq (18, 5.5)	
		$Hf[CH=CHCH_3$	1.88 dd (5.5, 1.5)	
$Cp_2^*Zr(CH=CHCH_2CH_3)_2$ (**6**)		$C_5(CH_3)_5$	1.78 s	
		$ZrCH=CHCH_2CH_3$	5.85 d (19)	
		$ZrCH=CHCH_2CH_3$	5.27 dt (19, 5.5)	
		$ZrCH=CHCH_2CH_3$	2.13 qd (7, 5.5)	
		$ZrCH=CHCH_2CH_3$	1.11 t (7)	

Compound	IR (cm⁻¹)	Assignment	¹H NMR δ (J)	¹³C NMR δ (J)
Cp*₂Zr(H)(C(CH₃)=CHCH₃) (7a) [e,f]	ν(C=C) 1513 ν(Zr–H) 1565	C₅(CH₃)₅	1.83 s	12.0 q (126)
		C₅(CH₃)₅		114.7 s
		ZrC(CH₃)=CHCH₃		191.0 s
		ZrC(CH₃)=CHCH₃	2.26 s, br	11.4 q (120)
		ZrC(CH₃)=CHCH₃	1.71 d (4.5)	17.5 qd (121, 16)
		ZrC(CH₃)=CHCH₃	3.65 m	86.5 dqd (120, 11, 5.5)
		Zr–H	4.29 d (4.0)	
Cp*₂Hf(H)(C(CH₃)=CHCH₃) (7b) [e,f]	ν(C=C) 1486 ν(Hf–H) 1568 ν(Hf–D) 1123	C₅(CH₃)₅	1.90 s [g]	11.9 q (126) [g]
		C₅(CH₃)₅	1.91 s [h]	13.2 q (126) [h]
				115.1 s
				116.6 s
		HfC(CH₃)=CHCH₃		198.6 s
				201.7 s
		HfC(CH₃)=CHCH₃	2.14 s, br	9.9 q (126)
			0.94 s, br	11.7 q (126)
		HfC(CH₃)=CHCH₃	1.73 d (5.8)	19.2 qd (124, 13.5)
			1.73 '	30.7 q (125)
		HfC(CH₃)=CHCH₃	3.80 m	93.6 d (130)
			4.89 m	125.8 d (143)
		Hf–H	9.59 d (3.4)	
			12.04 s	
Cp*₂ZrCH₂CH(CH₃)CH=C(CH₃) (8) [e,f]	ν(C=C) 1554	C₅(CH₃)₅	1.80 s	12.0 q (126)
		C₅(CH₃)₅	1.83 s	11.4 q (126)
				118.2 s
				118.4 s
		ZrCH(H)CH(CH₃)	0.02 ddd (13, 7.9, 2.4)	53.3 t (122)
		ZrCH(H)CH(CH₃)	1.27 dd (13, 8.8)	
		ZrCH(H)CH(CH₃)	2.33 m	
		ZrCH(H)CH(CH₃)	1.22 d (6.6)	32.2 d (122)
		ZrC(CH₃)=CH	6.07 d (1.5)	26.7 qd (123, 12)
		ZrC(CH₃)=CH	1.69 s	138.0 d (139)
		ZrC(CH₃)=CH		29.1 q (124)
				193.6 s

TABLE 1 (continued)

Compound	IR	NMR (Chemical shift, multiplicity (coupling constants))		
		Assignment	¹H	¹³C
Cp*₂ZrCH₂CH(CH₃)C(CH₃)=CH (9) ^{e,f,l}	ν(C=C) 1555	C₅(CH₃)₅	1.79 s	11.7 q (126)
			1.83 s	11.7 q (126)
		C₅(CH₃)₅		118.0 s
				118.2 s
		ZrCH(H)CH(CH₃)	−0.17 dd (13, 7.4)	57.7 t (119)
		ZrCH(H)CH(CH₂)	1.35 dd (13, 8.8)	
		ZrCH(H)CH(CH₃)	2.51 m	41.6 dd (127, 10)
		ZrCH(H)CH(CH₃)	1.24 d (7.0)	26.5 qd (125, 5)
		ZrCH=C(CH₃)	5.49 s	184.3 d (128)
		ZrCH=C(CH₃)	1.80 s	27.3 q (120)
		ZrCH=C(CH₃)		151.3 s
Cp*₂Zr(CH=CHCH₃)(C≡CCH₃) (11) ^{e,k}	ν(C=C) 1566	C₅(CH₃)₅	1.91 s	12.2 q (127)
	ν(C≡C) 2095	C₅(CH₃)₅		119.2 s
		ZrCH=CHCH₃	5.98 dq (18.5, 1)	192.3 ddq (122, 6, 6)
		ZrCH=CHCH₃	5.49 dq (18.5, 6.0)	130.1 ddq (152, 6, 6)
		ZrCH=CHCH₃	1.90 dd (6.0, 1.4)	124.4 qdd (124, 12, 8)
		ZrC≡CCH₃	1.77 s	5.8 q (127)
		ZrC≡CCH₃		110.6 q (10)
		ZrC≡CCH₃		140.3 q (4)
Cp*₂Zr(CH=C(CH₃)CH(CH₃)₂)(C≡CCH₃) ^{e,f}		C₅(CH₃)₅	1.04 s	12.2 q (127)
		C₅(CH₃)₅		119.3 s
		ZrCH=C(CH₃)CH(CH₃)₂	4.81 s	187.6 d (106)
		ZrCH=C(CH₃)CH(CH₃)₂	l	11.3 q (125)
		ZrCH=C(CH₃)CH(CH₃)₂	2.77 sep (7)	36.5 d (132)
		ZrCH=C(CH₃)CH(CH₃)₂	1.16 d (7)	22.6 qd (125, 5)
		ZrCH=C(CH₃)CH(CH₃)₂		l
		ZrC≡CCH₃		5.8 q (129)
		ZrC≡CCH₃	l	111.5 s
		ZrC≡CCH₃		l

	δ(¹H)	δ(¹³C)
Cp₂*ZrO(CH₃CH=CH)C=C(CH=CHCH₃)O (14a)ᵉ	ν(C=C) 1636, 1523	
C₅(CH₃)₃	1.85 s	10.8 q (126)
C₅(CH₃)₃		121.8 s
ZrOCCH=CHCH₃		148.2 s
ZrOCCH=CHCH₃	6.46 dq (14.6, 1.2)	126.4 ddq (147, 7, 2)
ZrOCCH=CHCH₃	5.96 dq (14.6, 7.0)	117.5 ddq (156, 14. 7)
ZrOCCH=CHCH₃	1.91 dd (17.0, 1.2)	18.6 qdd (125, 12, 6)
Cp₂*HfO(CH₃CH=CH)C=C(CH=CHCH₃)O (14b)	ν(C=C) 1631, 1528	
C₅(CH₃)₅	1.87 s	10.8
C₅(CH₃)₅		120.7
HfOCCH=CHCH₃		146.7
HfOCCH=CHCH₃	6.45 dq (15.0, 1.0)	126.5
HfOCCH=CHCH₃	5.93 dq (15.0, 6.2)	117.3
HfOCCH=CHCH₃	m	18.6
Cp₂*Zr(H)(OC=CHCH(CH₃)CH=C(CH₃)) (15) a b c d e f g		
C₅(CH₃)₅	1.95 s	11.7 q (127)
C₅(CH₃)₅		118.4 s
a		{ 138.7 s
f		{ 162.6 s
b	4.95 m (1)	{ 107.5 d (162)
e	5.98 m (1)	{ 134.8 d (158)
d	1.18 d (7.5)	{ 12.6 q (127)
g	1.90 s	{ 16.9 q (130)
c	3.06 qm (7.5, 1)	41.2 d (124)
Zr–H	6.12 s	
Cp₂*Zr(H)(OC=CHCH(CH₃)C(CCH₃)=CH) (16) a b c d e f g		
C₅(CH₃)₅		1.93 s 11.7 q (126)
C₅(CH₃)₅		118.3 s
a		149.3 s
e		162.0 s
b	4.84 m (1)	{ 103.4 d (165)
g	5.77 s	{ 128.8 d (160)
d	1.12 d (7.5)	{ 11.0 q (127)
f	1.68 s	{ 14.6 q (126)
c	2.75 dq (7.5, 1)	46.0 d (122)
Zr–H	6.28 s	

(continued)

TABLE 1 (continued)

Compound	IR	NMR (Chemical shift, multiplicity (coupling constants))		
		Assignment	^{1}H	^{13}C
$Cp^{\star}_2Zr(H)(\eta^3\text{-}CH_2CHCHCH_3)$ (17a)[n]	$\nu(\pi\text{-allyl})$ 1530	$C_5(CH_3)_5$	1.81 s	
	$\nu(Zr\text{-}H)$ 1575	$Zr(\eta^3\text{-}CH_2CHCHCH_3)$	3.81 dt (16, 11)	
		$Zr(\eta^3\text{-}CH_2CHCHCH_3)$		
		$Zr(\eta^3\text{-}CH_2CHCHCH_3)$	0.80–2.80 m, br	
		$Zr(\eta^3\text{-}CH_2CHCHCH_3)$		
		$Zr\text{-}H$		
$Cp^{\star}_2Hf(H)(\eta^3\text{-}CH_2CHCHCH_3)$ (17b)[o]		$C_5(CH_3)_5$	1.86 s	
		$Hf(\eta^3\text{-}CH_2CHCHCH_3)$	3.75 dt (16, 11)	
		$Hf(\eta^3\text{-}CH_2CHCHCH_3)$		
		$Hf(\eta^3\text{-}CH_2CHCHCH_3)$	0.80–2.90 m, br	
		$Hf(\eta^3\text{-}CH_2CHCHCH_3)$		
		$Hf\text{-}H$	4.24 s, br	
$Cp^{\star}_2ZrCH_2CH(CH_2CH_3)C(CH_3)\overline{=C(CH_3)}$ (18)[e,f]	$\nu(C=C)$ 1554	$C_5(CH_3)_5$	1.79 s	11.3 q (126)
		$C_5(CH_3)_5$	1.84 s	11.9 q (126)
				118.6 s
				118.7 s
		$ZrCH(H)CH(CH_2CH_3)$	−0.13 dd (13, 7.5)	54.7 td (117, 4)
		$ZrCH(H)CH(CH_2CH_2)$	1.35 dd (13, 8.5)	
		$ZrCH_2CH(CH_2CH_3)$	m	32.0 dt (128, 2)

Compound	Assignment	^{1}H	^{13}C	IR
	$ZrCH_2CH(CH_2CH_3)$	m	11.1 t (126)	
	$ZrCH_2CH(CH_2CH_3)$	1.12 t (7.0)	11.8 q (126)	
	$ZrC(CH_3)=C(CH_3)$	1.29 s	17.5 q (124)	
	$ZrC(CH_3)=C(CH_3)$	1.63 s	19.8 q (122)	
	$ZrC(CH_3)=C(CH_3)$		185.7 s	
	$ZrC(CH_3)=C(CH_3)$		144.6 s	
$Cp_2^*Zr(C{\equiv}CCH_3)_2$ (**20a**)	$C_5(CH_3)_5$	2.05 s	12.5	$\nu(C{\equiv}C)$ 2090
	$C_5(CH_3)_5$		120.0	
	$ZrC{\equiv}CCH_3$	1.77 s	6.0	
	$ZrC{\equiv}CCH_3$		112.9	
	$ZrC{\equiv}CCH_3$		40.9	
$Cp_2^*Hf(C{\equiv}CCH_3)_2$ (**20b**)[p]	$C_5(CH_3)_5$	2.07 s	12.4	$\nu(C{\equiv}C)$ 2102
	$C_5(CH_3)_5$		118.6	
	$ZrC{\equiv}CCH_3$	1.82 s	6.2	
	$ZrC{\equiv}CCH_3$		116.7	
	$ZrC{\equiv}CCH_3$		149.8	

[a] ^{1}H (90 MHz) and ^{13}C (22.5 MHz) NMR spectra taken in benzene-d_6 at ambient temperature unless otherwise noted. Chemical shifts are reported in δ relative to internal TMS or by reference to residual protons or carbons in the solvent. Coupling constants are reported in Hz. [b] IR spectra obtained in Nujol mulls unless otherwise noted. Values given in cm^{-1}. [c] Ref. 13. [d] ^{1}H and IR data from ref. 10. [e] ^{13}C NMR spectrum obtained at 125 MHz. [f] ^{1}H NMR spectrum obtained at 500 MHz. [g] In each set of lines the first entry is for major ($\sim 90\%$) isomer ($\sim 90\%$) isomer. [h] The second entry is for the minor ($\sim 10\%$) isomer. [i] This resonance was only identified when the integration of the ^{1}H-decoupled ^{2}H resonance at δ 1.73 equalled the sum of the integrations for δ 2.14 and 0.94 in the spectrum of **7b**-d_6, and no other resonance was observed in the spectrum. [j] IR spectrum taken in C_6H_6. [k] ^{1}H data from ref. 23. [l] These may not be definitively assigned: 1.79 s and 1.80 s for CH_3; 141.1 s and 147.6 s for quaternary carbons. [m] Not observed. [n] Ref. 18. [o] Toluene-d_8. [p] IR spectrum taken in C_6D_6.

The yield is quantitative by NMR, with the high solubility of these complexes reducing the isolated yields. Compound **5a** is stable at low temperature, but at room temperature rearranges in solution ($t_{1/2}$ 9.1 h at 24°C) to form zirconacyclopentenes, as described in detail in the next section.

Infrared and nuclear magnetic resonance spectra are consistent with the formulation of **5a** as a bis(propenyl) complex: a C=C stretch of medium intensity is observed at 1570 cm^{-1} and ^{13}C NMR data show the downfield shift and reduced ^{13}C$-^1$H coupling constant expected for the carbons nearest the Lewis acidic metal center [17] (δ 191.5 ppm, ^1J(CH) 114 Hz) and more typical sp^2-carbon values for the β-carbons [18] (δ 130.4 ppm, ^1J(CH) 148 Hz). These assignments are supported by deuterium labeling experiments. By treating **1a** with 1-d-propyne and Cp_2^*ZrD$_2$ (**1a**-d_2) with perprotio propyne (eqs. 4 and 5), it is possible to specifically label the α and β positions.

$$Cp_2^* ZrH_2 \ + \ 2\ DC{\equiv}CCH_3 \ \longrightarrow \ Cp_2^*Zr \qquad\qquad (4)$$

(**1a**) (**5a**-($\alpha\ d$)$_2$)

$$Cp_2^* ZrD_2 \ + \ 2\ HC{\equiv}CCH_3 \ \longrightarrow \ Cp_2^*Zr \qquad\qquad (5)$$

(**1a** - d_2) (**5a**-($\beta\ d$)$_2$)
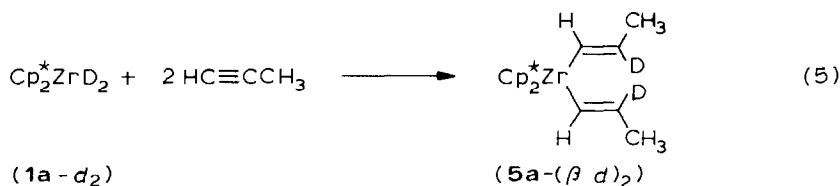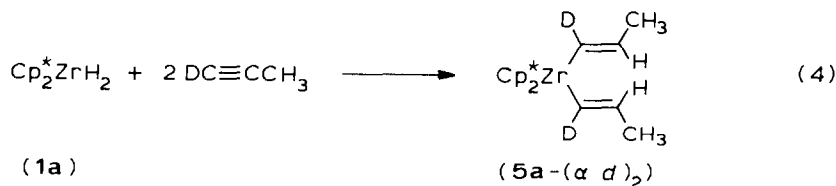
Compound **5b** can be isolated as a colorless microcrystalline solid in good yield (60%) from petroleum ether solutions. Its infrared and NMR data are analogous to that for the zirconium complex **5a** (Table 1). However, ^{1}H NMR shows that an impurity, whose identify is unknown, comprises approximately 10% of the isolated product [17]. Repeated recrystallization attempts have failed to further purify **5b**. Unlike **5a**, the hafnium complex **5b** is stable in solution at 80°C; no change is observed in the NMR spectrum for days at 80°C until decomposition begins. Moreover, the formation of **5b** is notably slower than that of its zirconium analogue **5a**. Signals assignable to the monoinsertion product Cp_2^*Hf(H)(CH=CHCH$_3$) can be observed by ^{1}H NMR, even at room temperature. The insertion of propyne into the second Hf–H bond is still sufficiently fast, however, to preclude clean isolation of this intermediate even when a single equivalent of propyne is utilized.

The reaction of Cp_2^*ZrH$_2$ (**1a**) with 1-butyne proceeds analogously to the reaction with propyne, yielding only the bisinsertion product Cp_2^*Zr(CH=CHCH$_2$CH$_3$)$_2$ (**6**) with no observation of the monoinsertion intermediate (eq. 6). Compound **6** is very

$$Cp_2^* ZrH_2 \ + \ 2\ HC{\equiv}CCH_2CH_3 \ \longrightarrow \ Cp_2^*Zr \qquad\qquad (6)$$

(**1a**) (**6**)

soluble; its isolation as a pale yellow solid requires evaporation of the solvent. The NMR data are again consistent with a *cis* addition of Zr–H to the alkyne (^3J(HH) 21 Hz, Table 1). As expected, the reactivity of the bis(butenyl)zirconium complex 6 is analogous to that of the bis(propenyl)zirconium complex 5a (vide infra).

The reactions of $Cp_2^*MH_2$ (1a and 1b) with 2-butyne, however, proceed quite differently, yielding only the monoinsertion products $Cp_2^*M(H)(C(CH_3)=CHCH_3)$ (7a and 7b) (eq. 7). The addition is assumed to be *cis* by analogy to the preceding reactions; however, this assumption could not be confirmed by ^1H NMR spectrometry. Apparently the internal alkenyl ligand is sufficiently sterically demanding to

$$Cp_2^*MH_2 \; + \; H_3CC{\equiv}CCH_3 \; \longrightarrow \; Cp_2^*M \overset{\diagup}{\underset{\overset{|}{H}}{}} \qquad (7)$$

(M = Zr, 1a ,　　　　　　　　(M = Zr, 7a ,

　M = Hf, 1b)　　　　　　　　　M = Hf, 7b)
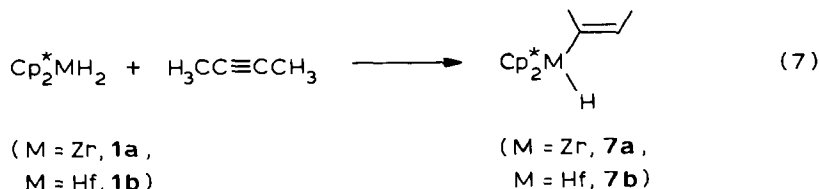
prevent the insertion of a second molecule of 2-butyne. The reactions induced under more forcing conditions will be discussed in a subsequent section.
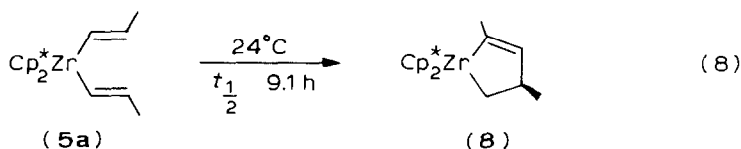
The ^1H and ^{13}C NMR data for compound 7b (Table 1) indicate that it exists in two isomeric forms in a 90/10 ratio at room temperature. The ratio decreases reversibly to 85/15 at 80°C. The ratio of isomers changes slightly (88/12) when the deuterated analogs $Cp_2^*Hf(D)(C(CH_3)=CDCH_3)$ (7b-d_2) and Cp_2^*-Hf(H)(C(CD_3)=CHCD_3) (7b-d_6) are formed from $Cp_2^*HfD_2$ (1b-d_2) and 2-butyne and $Cp_2^*HfH_2$ (1b) and 2-butyne-d_6, respectively.

The ^1H and ^{13}C NMR data for 7a and the major isomer of 7b (Table 1) are unusual by comparison to the alkenyl derivatives with only H at the α position (2a, 2b, 5a, 5b, and 6). The metal–hydride ^1H NMR signal is significantly farther upfield for 7a and the major isomer of 7b as compared to 2a and 2b. The metal–hydride resonance of the minor isomer of 7b, in contrast, is very close to that of 2b. Similarly, the ^{13}C NMR spectra for 7a and the major isomer of 7b show the β-carbon significantly upfield with a large reduction in the coupling constant (^1J(CH) 120 Hz for 7a, 130 Hz for 7b-major). The α-carbon resonance for 7a and 7b and the β-carbon resonance for 7b-minor, in contrast, appear at positions similar to those of 2a, 2b, 5a, 5b, and 6. The significance of these results will be considered further in the Discussion section.

Reactivity of the bis(alkenyl) derivatives of permethylzirconocene and permethylhafnocene

(1) Isomerization reactions. The thermal stability of coordinatively unsaturated, 16-electron compounds of the form $Cp_2^*MR_2$ (M = Zr, Hf; R = alkyl) is well documented [9]. The increased stability of an alkenyl hydride over an alkyl hydride complex had been noted [10]. Thus it was surprising to observe that the bis(alkenyl) derivatives of permethylzirconocene were not stable at room temperature in hydrocarbon solutions, but rather rearranged to zirconacyclopentenes.

The bis(propenyl) compound, $Cp_2^*Zr(CH=CHCH_3)_2$ (5a), reacts at 24°C with a half-life of 9.1 h to form zirconacyclopentene 8 (eq. 8).

$$\text{Cp}_2^*\text{Zr} \xrightarrow[t_{\frac{1}{2}} \quad 9.1\text{ h}]{24^\circ\text{C}} \text{Cp}_2^*\text{Zr} \qquad\qquad (8)$$

$$(5a) \qquad\qquad\qquad\qquad\qquad (8)$$

Interestingly, this zirconacyclopentene **8** is also unstable, rearranging over weeks at room temperature and more rapidly at 78°C ($t_{1/2}$ 6.5 h) to yield a second, isomeric, zirconacyclopentene **9** (eq. 9). Both products have been isolated as bright yellow,

$$\text{Cp}_2^*\text{Zr} \xrightarrow[t_{\frac{1}{2}} \quad 6.5\text{ h}]{78^\circ\text{C}} \text{Cp}_2^*\text{Zr} \qquad\qquad (9)$$

$$(8) \qquad\qquad\qquad\qquad\qquad (9)$$
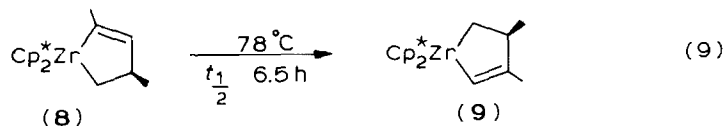
microcrystalline solids and have been characterized by infrared and NMR spectroscopies (Table 1) and microanalyses. Deuterium labeling, from the rearrangements of **5a**-$(\alpha d)_2$ and **5a**-$(\beta d)_2$ (vide infra), has allowed unambiguous assignment of all resonances. As was noted for the previously described compounds, the ^{13}C NMR data are most useful. The position of the resonance of each carbon that is immediately adjacent to zirconium (e.g., δ 193.6 and 53.3 ppm in **8**) is shifted downfield relative to its next neighbor (δ 138.0 and 32.2 ppm) [15].

Two alternate isomeric zirconacyclopentenes with a methyl group on the α sp^3-carbon are not observed. Their absence probably results from unfavorable steric interactions of the CH_3 group with the bulky Cp^* ligands. Indeed, to our knowledge, no stable example of a metallacyclopentane or metallacyclopentene derivative of $[Cp_2M]$ ((M = Ti, Zr, Hf) with alkyl substitution at the sp^3-hybridized α-carbon has been isolated. Internal olefins isomerize to terminal olefins prior to coupling to form five-membered rings [4a,18]. Only Whitesides and co-workers have reported such a compound, $Cp_2TiCH(Me)(CH_2)_2CH_2$, formed from the reaction of Cp_2TiCl_2 with 1,4-dilithiopentane, but they report its decomposition above -45°C [19].

Our overall reaction, then, involves the very rapid formation of an isolable kinetic product, the bis(propenyl) compound **5a**, that subsequently rearranges to a second cleanly isolable kinetic product, the zirconacyclopentene **8**, which in turn forms the thermodynamic zirconacyclopentene product **9** (eqs. 3, 8, and 9). Compound **9** is expected to be very stable, as numerous examples of related species have been reported in the literature [20]. Although zirconacyclopentene **8** can be cleanly isolated from petroleum ether solution, ^{1}H NMR spectra taken to follow the isomerization of **5a** in benzene-d_6 reveal that 11% of the thermodynamic product **9** is present in these solutions. Since rearrangement of **8** to **9** is slow at room temperature (vide supra), this observation suggests a common intermediate and allows us to calculate a transition state energy difference of 1.2(1) kcal mol^{-1} in the formation of **8** and **9** [21].

A mechanism that accounts for these observations is shown in Scheme 1. The propyne coordination and insertion steps leading to **5a** must all be rapid since no intermediates are detected even at -78°C. The common intermediate in the formation of zirconacyclopentenes **8** and **9** is the zirconium(II)-η^2-propyne species

$[Cp_2^* Zr(HC\equiv CCH_3)]$ **(10)**, formed via β-hydrogen elimination from one of the propenyl ligands to yield the 18-electron intermediate $[Cp_2^* Zr(CH= CHCH_3)(H)(HC\equiv CCH_3)]$, followed by reductive elimination of propene. The competition between faster insertion of propyne to generate **5a** and induced reductive elimination of propene yielding **10** is entirely analogous to the ethylene-induced reductive elimination of isobutane from $Cp_2^* Zr(H)(CH_2CHMe_2)$ [9c].
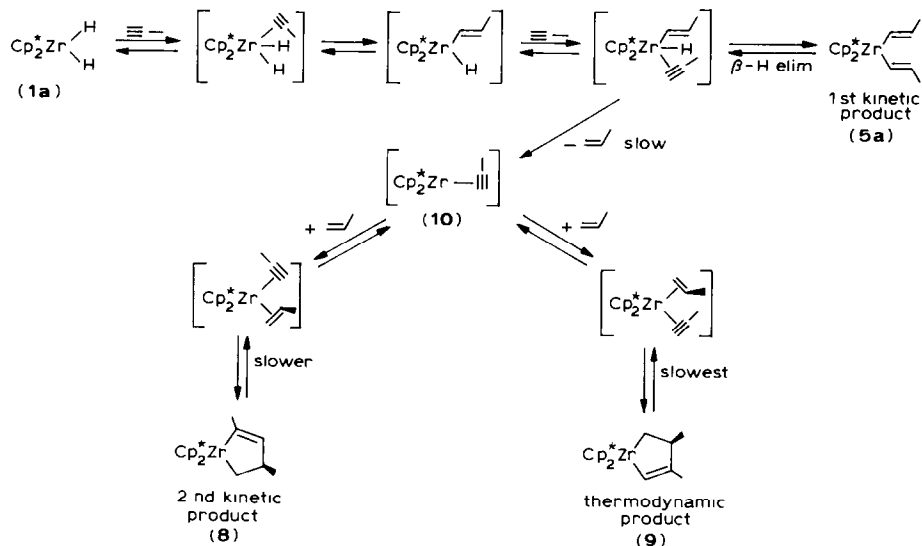
SCHEME 1

The zirconium-propyne intermediate **10** has precedent in the stable, isolated η^2-alkyne derivatives $Cp_2^* Ti(CH_3C\equiv CCH_3)$, $Cp_2^* Ti(PhC\equiv CPh)$, and $Cp_2^* Zr$-$(PhC\equiv CPh)$ [22]. Its intermediacy is also strongly suggested by the reactions of **5a** and **8** in the presence of excess alkyne. Both the bis(propenyl) compound **5a** and the kinetic metallacyclopentene **8** react with excess propyne (eqs. 10 and 11) to form the

same propenyl-propynyl species (11) that is formed from the reaction of the known $[Cp_2^* Zr^{II}]$ precursor $\{Cp_2^* ZrN_2\}_2 N_2$ with propyne (eq. 12) [23].

$$Cp_2^* Zr + HC\equiv CCH_3 \longrightarrow Cp_2^* Zr \qquad (13)$$

$$(9)$$

In contrast, the thermodynamic zirconacyclopentene 9 reacts quite differently with propyne (eq. 13), giving a product (identified by NMR) that does not arise from intermediate 10 but rather from addition of propyne across the zirconium–sp^3-carbon bond in a manner similar to the reactions of these complexes with H_2 (vide infra).

Studies with the deuterium-labeled compounds provide further supporting evidence for the proposed mechanism. $Cp_2^* Zr(CH=CDCH_3)_2$, 5a-$(\beta d)_2$, reacts in the presence of propyne to yield 1,2-dideuteriopropene and 11-d_0 according to Scheme 2. The steps leading to the formation of the Zr^{II} intermediate 10 are those of our

$$(5a-(\beta d)_2) \qquad (11) \qquad (10)$$

SCHEME 2

proposed mechanism (Scheme 1). The steps from the formation of 10 onwards are those proposed for the reaction of $\{Cp_2^* ZrN_2\}_2 N_2$ with propyne (eq. 12) [23], and hence any compound with access to intermediate 10 will follow the same path. The different reactivity of the thermodynamic zirconacyclopentene 9 suggests that 10 is not accessible from 9, again speaking to the high thermodynamic stability of this zirconacyclopentene.

In the absence of propyne, 5a-$(\beta d)_2$ yields the specifically labeled zirconacyclopentene (8-d_2)$_A$ (eq. 14), the product expected for the reaction of intermediate 10

$$Cp_2^* Zr \longrightarrow Cp_2^* Zr \qquad (14)$$

$$(5a-(\beta d)_2) \qquad ((8-d_2)_A)$$

with free cis-1,2-dideuteriopropene (Schemes 1 and 2). Similarly, $Cp_2^*Zr(CD=CHCH_3)_2$ ($5a$-$(\alpha d)_2$) yields the doubly labeled zirconacyclopentene (8-d_2)$_B$ (eq. 15).

$$\text{(15)}$$
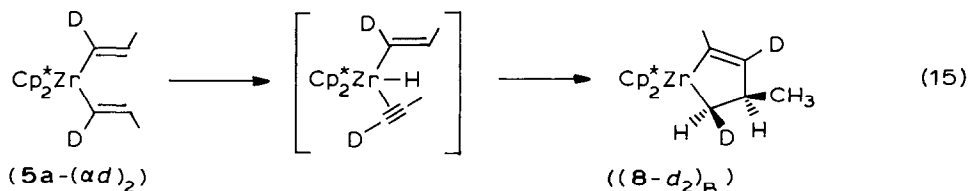
The products of the rearrangements of perprotio $5a$ and 8 in the presence of propene-d_6 indicate that propene is indeed released from the coordination sphere of zirconium. In the presence of a two-fold molar excess of propene-d_6 at 24°C, $5a$ yields 8 with propene-d_6 incorporated in 90% of the product (eq. 16). At 78°C, 8

$$\text{(16)}$$
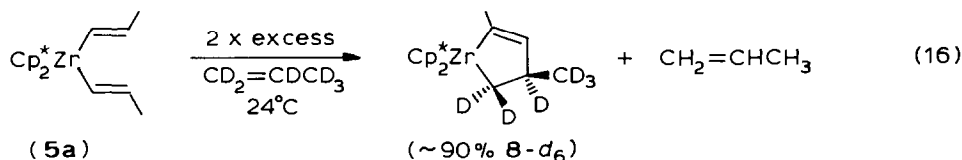
yields 9 with propene-d_6 incorporated in 80% of the product (eq. 17). Propene-d_6 is incorporated into zirconacyclopentene 8 faster than 8 isomerizes to 9, as evidenced by liberation of 50% of the possible perprotio propene before 10% of 8 has rearranged to 9. This result is consistent with the proposal of the common intermediate 10 reacting to produce the kinetic product 8 faster than the thermodynamic product 9. No exchange of propene-d_6 into 9 is observed even after one day at 80°C,

$$\text{(17)}$$
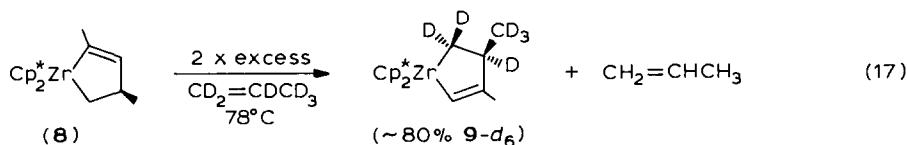
again indicating that the reversion of 9 to 10 has a much higher activation barrier than that of 8 to 10.

The availability of $5a$, $5a$-$(\beta d)_2$ and $5a$-$(\alpha d)_2$ has permitted measurement of the kinetics for the rearrangements of the bis(propenyl) complex $5a$ and the zirconacyclopentene 8, including deuterium isotope effects and activation barriers [24]. The isomerizations of $5a$ to 8 and 8 to 9 were first-order in loss of $5a$ and 8, respectively, to three half-lives (Figs. 1 and 2). The isomerization of the bis(propenyl) complex $5a$ to zirconacyclopentene 8 has a half-life of 9.1 h at 24°C, corresponding to k_{obs} $2.1(2) \times 10^{-5}$ s^{-1} and $\Delta G^{\ddagger}$(297 K) 23.7(2) kcal mol^{-1}. When deuterium replaces hydrogen in the β positions of $5a$, the reaction is slowed significantly, yielding $k_H/k_D = 4.9(5)$. When deuterium replaces hydrogen in the α positions, however, the reaction rate is not significantly changed ($k_H/k_D = 1.03(10)$). The magnitudes of

these isotope effects indicate the β carbon–hydrogen bond is indeed being broken as **5a** rearranges.

Similarly, the isomerization of zirconacyclopentene **8** to zirconacyclopentene **9** has a half-life of 6.5 h at 78°C, corresponding to k_{obs} $3.0(3) \times 10^{-5}$ s^{-1} and $\Delta G^{\ddagger}$ (351 K) 27.9(3) kcal mol^{-1}, comparable to the values found for the ring cleavage of
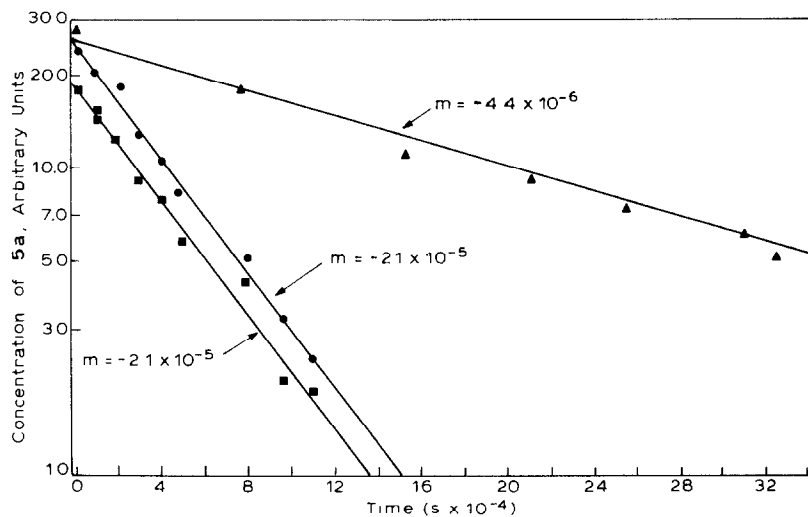
Fig. 1. The rearrangement of **5a**: kinetic plots demonstrating the first-order nature of the loss of **5a** (●), **5a**-$(\alpha d)_2$ (■), and **5a**-$(\beta d)_2$ (▲) at 24°C. The loss of **5a**, **5a**-$(\alpha d)_2$, and **5a**-$(\beta d)_2$ was monitored by measuring the peak height of the Cp* resonance relative to the peak height of internal TMS.
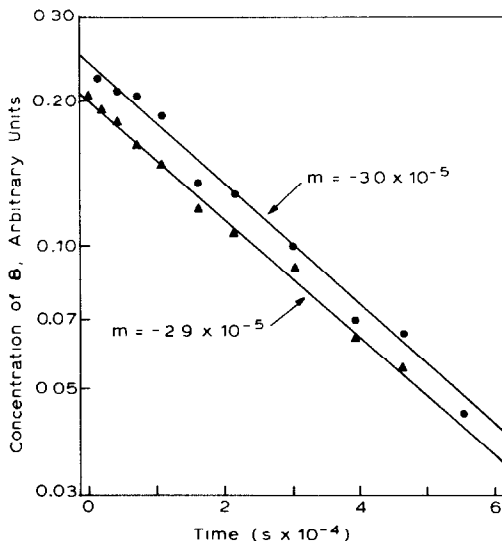

Fig. 2. The rearrangement of **8**: kinetic plots demonstrating the first-order nature of the loss of **8** (●) and $(8\text{-}d_2)_A$ (▲) at 78°C. The loss of **8** and $(8\text{-}d_2)_A$ was monitored by measuring the peak height of the vinylic proton relative to the peak height of residual protons of C_6D_6.

zirconaindans [20a]. When $(8\text{-}d_2)_A$ is thermolyzed the rearrangement proceeds slightly more slowly, yielding $k_H/k_D = 1.07(10)$. Although this value is not statistically different from unity, the direction (> 1) is consistent with that expected for a rate-determining ring cleavage in which a decrease in p-character ($sp^3 \rightarrow sp^2$) occurs for the carbons bearing the deuteriums [26]. Similar measurements were not undertaken for $(8\text{-}d_2)_B$, since no NMR resonance is sufficiently isolated to monitor.

In order to ascertain whether free propene had any effect on the rate of isomerization of 5a, zirconacyclopentene formation was monitored in the presence of 0, 2.1 and 9.7 molar equivalents of excess propene. In each case, the reaction is first-order in loss of the bis(propenyl) complex 5a to three half-lives (Fig. 3). Significantly, the rate at 28°C did not change with increasing amounts of free propene, yielding k_{obs} 2.9×10^{-5} s^{-1} (no added propene), 3.3×10^{-5} s^{-1} (2.1 molar equivalents of propene), and 2.9×10^{-5} s^{-1} (9.7 molar equivalents of propene), for an average k_{obs} $3.0(2) \times 10^{-5}$ s^{-1}. Thus, free propene is not involved in the rate-determining step, although the experiments utilizing propene-d_6 (vide supra) show that propene is liberated in the formation of the zirconacyclopentenes 8 and 9.

In contrast, the rate of isomerization of zirconacyclopentene 8 is found to increase linearly with the concentration of added propene. The apparent rate constants, k_{obs} 5.9×10^{-4} s^{-1} (no added propene), 6.7×10^{-5} s^{-1} (2.2 molar equivalents of propene), and 8.7×10^{-5} s^{-1} (8.3 molar equivalents of propene), fit the equation
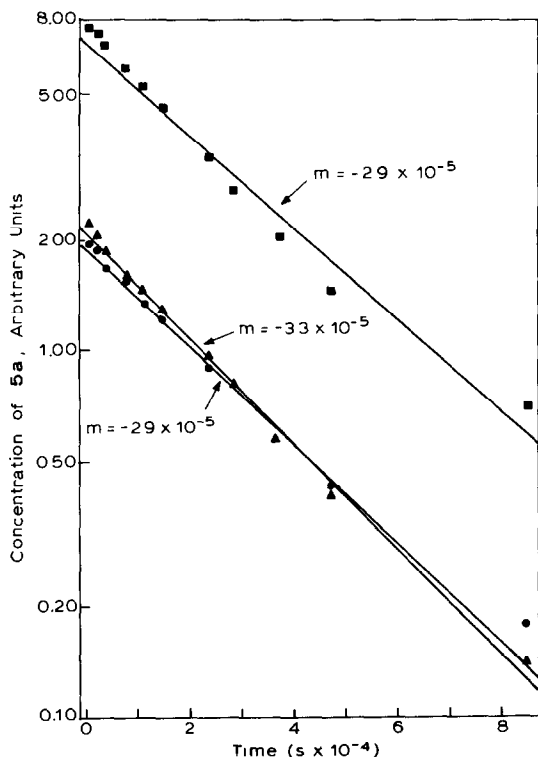

Fig. 3. The rearrangement of 5a in the presence of propene: kinetic plots demonstrating the first-order nature of the loss of 5a in the presence of 0 (●), 2.1 (▲), and 9.7 (■) molar equivalents of propene at 28°C. The loss of 5a was measured as described for Fig. 1.

$k_{obs} = k + k'$[propene], where $k = 5.9(6) \times 10^{-5}$ s^{-1} and $k' = 2.1(2) \times 10^{-5}$ l mol^{-1} s^{-1} [25b]. Thus, free propene catalyzes (albeit rather poorly) the isomerization of zirconacyclopentene **8** to zirconacyclopentene **9**, and will therefore influence the results of the experiments conducted in the presence of propene-d_6. However, the unimolecular transformation of **8** to **9** competes effectively at the concentration of propene-d_6 (~ 0.4 M) utilized in these experiments (k 5.9×10^{-5} s^{-1} vs. k'[propene-d_6] $\cong 8.4 \times 10^{-6}$ s^{-1}), so that the high level of propene-d_6 incorporation and, especially, the observation that 50% of the available perprotio propene is released before 10% of **8** has been lost indicate that loss of propene to form intermediate **10** is a key feature in the isomerization of **8** to **9**.

The bis(butenyl) complex Cp$_2^*$Zr(CH=CHCH$_2$CH$_3$)$_2$ (**6**) behaves analogously to the bis(propenyl) complex **5a**, rearranging to zirconacyclopentanes **12** and **13** (eq. 18), with **13** as the thermodynamic, and ultimately only, product. The rate is

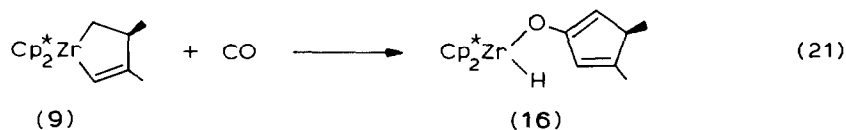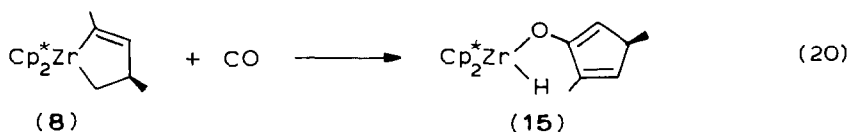(18)

(6)   (12)   (13)
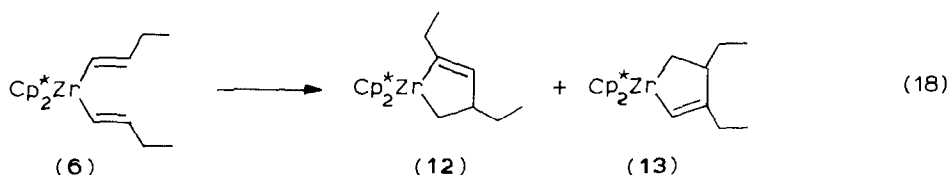
qualitatively similar to that observed for the isomerization of **5a**. However, the energy difference between the activation barriers for the kinetic ring **12** and the thermodynamic ring **13** is less, with **13** accounting for approximately one quarter of the initially observed ring products ($\Delta E_a \cong 0.6$ kcal mol^{-1}).

(2) Reactions with CO and H$_2$. Facile insertion of CO into Zr–C and Hf–C bonds has been previously observed for alkyl derivatives of permethylzirconocene and permethylhafnocene [9a,b]. Both the bis(propenyl) derivatives Cp$_2^*$Zr(CH=CHCH$_3$)$_2$ (**5a**) and Cp$_2^*$Hf(CH=CHCH$_3$)$_2$ (**5b**) react quickly with CO at room temperature to yield quantitatively (NMR) the purple enediolate derivative of permethylzirconocene (**14a**, eq. 19) and the red enediolate derivative of permethylhafnocene (**14b**, eq. 19). The stoichiometry of two mol CO/mol **5** is confirmed by

(19)

(M = Zr, **5a**;   (M = Zr, **14a**,
  M = Hf, **5b**)   M = Hf, **14b**)
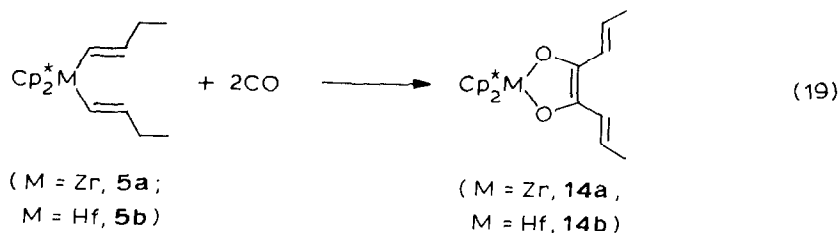
Toepler pump experiments. Unlike the alkyl analogues [9b,10], however, the mono-insertion product is never observed. The NMR and IR data (Table 1) are analogous to those observed in similar titanium [27], zirconium [4], and hafnium [10] species.

Both zirconacyclopentenes **8** and **9** react with one equivalent of CO at room temperature to yield orange dienolate-hydride derivatives **15** and **16** respectively (eqs. 20 and 21) in quantitative yield by NMR. The stoichiometry is confirmed by Toepler pump experiments. The reactivity is analogous to that of bis(pentamethyl-cyclopentadienyl)zirconacyclopentane, which produced an enolate-hydride upon re-

$$\text{Cp}_2^*\text{Zr} \diagdown \!\!\!\!\!\diagup + \text{CO} \longrightarrow \text{Cp}_2^*\text{Zr} \diagdown\!\!\!\!\!\diagup \quad (20)$$

$$(8) \qquad\qquad\qquad (15)$$

$$\text{Cp}_2^*\text{Zr} \diagdown\!\!\!\!\!\diagup + \text{CO} \longrightarrow \text{Cp}_2^*\text{Zr} \diagdown\!\!\!\!\!\diagup \quad (21)$$

$$(9) \qquad\qquad\qquad (16)$$

action with CO (eq. 22) [9b]. Compounds **15** and **16** have been characterized by NMR and IR, but have not been isolated. After weeks at room temperature,

$$\text{Cp}_2^*\text{Zr} \diagdown\!\!\!\!\!\diagup + \text{CO} \longrightarrow \text{Cp}_2^*\text{Zr} \diagdown\!\!\!\!\!\diagup \quad (22)$$
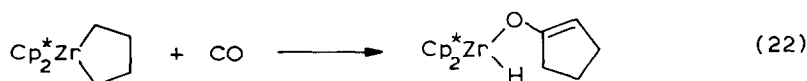
compounds **15** and **16** are observed to have undergone apparent sigmatropic [1,2]-hydrogen shifts in solution producing isomers of the original compounds. According to ^{13}C and ^{1}H NMR spectra, a single isomer results from the rearrangement of **15**. The data do not, however, define which of the two possible products is produced. The rearrangement of dienolate-hydride **16** is less clean and was not pursued.
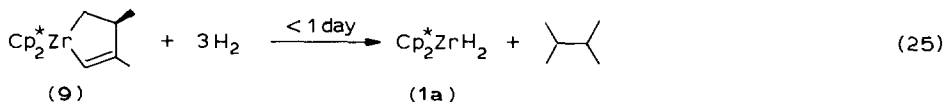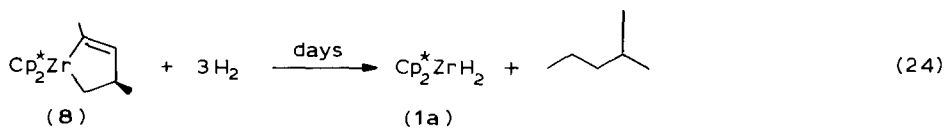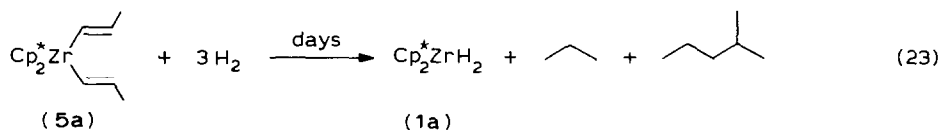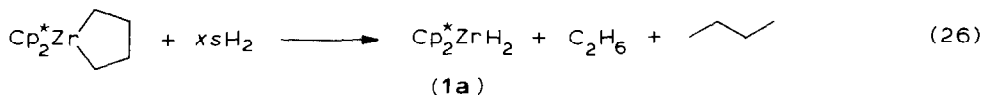
All the zirconium-alkenyl complexes **5a**, **8** and **9** react with excess dihydrogen, yielding $\text{Cp}_2^*\text{ZrH}_2$ and alkane (eqs. 23, 24 and 25).

$$\text{Cp}_2^*\text{Zr} \diagdown\!\!\!\!\!\diagup + 3\,\text{H}_2 \xrightarrow{\text{days}} \text{Cp}_2^*\text{ZrH}_2 + \diagup\!\!\!\!\!\diagdown + \diagup\!\!\!\!\!\diagdown\!\!\!\!\!\diagup \quad (23)$$

$$(5a) \qquad\qquad\qquad (1a)$$

$$\text{Cp}_2^*\text{Zr} \diagdown\!\!\!\!\!\diagup + 3\,\text{H}_2 \xrightarrow{\text{days}} \text{Cp}_2^*\text{ZrH}_2 + \diagup\!\!\!\!\!\diagdown\!\!\!\!\!\diagup \quad (24)$$

$$(8) \qquad\qquad\qquad (1a)$$

$$\text{Cp}_2^*\text{Zr} \diagdown\!\!\!\!\!\diagup + 3\,\text{H}_2 \xrightarrow{< 1\,\text{day}} \text{Cp}_2^*\text{ZrH}_2 + \diagup\!\!\!\!\!\diagdown\!\!\!\!\!\diagup \quad (25)$$

$$(9) \qquad\qquad\qquad (1a)$$

The hafnium-alkenyl complex **5b** does not appear to react with H_2, even after days at room temperature. The reaction of the bis(propenyl) compound **5a** with H_2 is sufficiently slow that a significant amount of rearrangement to zirconacyclopentene **8** occurs. Compound **8** then also reacts with H_2, so that a mixture of propane and 2-methylpentane is obtained. The reactions of zirconacyclopentenes **8** and **9** with H_2 differ somewhat from the reactions of the analogous zirconacyclopentane with H_2 (eq. 26) [23]. In the latter reaction, alkane products arise from both the zircona-

$$Cp_2^*Zr\langle\bigcirc \quad + \quad xsH_2 \quad \longrightarrow \quad Cp_2^*ZrH_2 \quad + \quad C_2H_6 \quad + \quad \diagup\diagdown\diagup \qquad (26)$$

$$(1a)$$

cyclopentane and the bis(olefin) forms of the compound (eq. 27). In the former reactions, the alkane products arise solely from the zirconacyclopentene form,

$$Cp_2^*Zr\langle \quad \rightleftarrows \quad Cp_2^*Zr\langle\bigcirc \qquad (27)$$
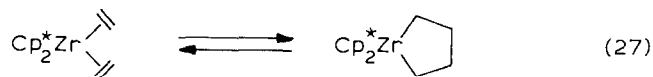
suggesting that the equilibrium between zirconacyclopentene and zirconium(olefin)(acetylene) lies much farther to the side of the zirconacyclopentene.

Reactivity of the mono(alkenyl) derivatives of permethylzirconocene and permethylhafnocene

The thermal stability of the monoinsertion products $Cp_2^* M(H)(CH{=}CHCMe_3)$ (M = Zr, **2a**; Hf, **2b**) has been previously described [10]. They are found to be more stable to reductive elimination and other decomposition reactions than the related alkylhydride complexes. The monoinsertion products that result from the reaction of 2-butyne with $Cp_2^* ZrH_2$ (**1a**) and $Cp_2^* HfH_2$ (**1b**), however, do not show this same stability.

$Cp_2^* Zr(H)(C(CH_3){=}CH(CH_3))$ (**7a**) rearranges at room temperature in both the solid and solution states. The rearrangement in solution occurs with first-order loss of **7a** to give the crotyl-hydride species **17a** (eq. 28) with a half-life of 19.3 h at 24°C, corresponding to k_{obs} $1.0(1) \times 10^{-5}$ s^{-1} (Fig. 4). The analogous hafnium compound, $Cp_2^* Hf(H)(C(CH_3){=}CH(CH_3))$ (**7b**), rearranges more slowly and less cleanly, yielding primarily the crotyl-hydride species **17b**. At room temperature, the rearrange-
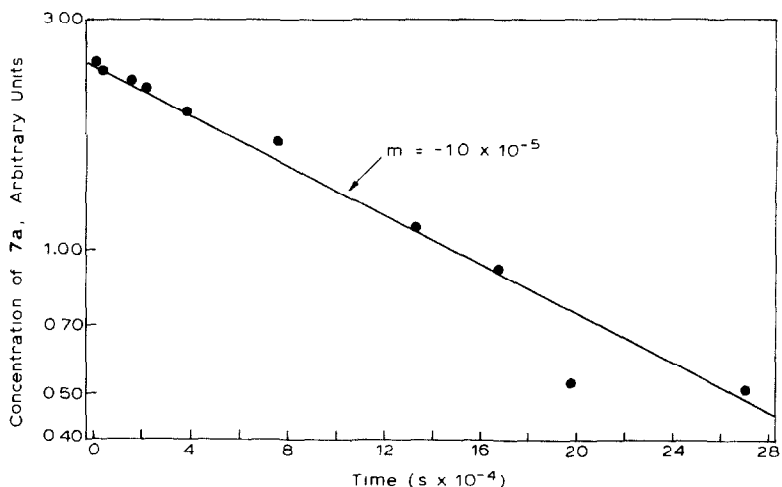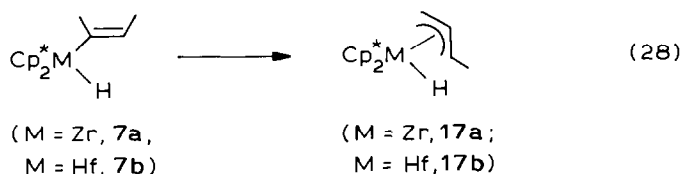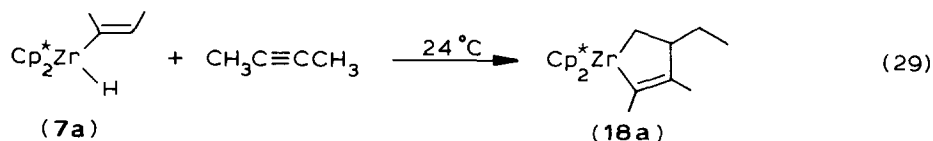

Fig. 4. The rearrangement of **7a**: kinetic plot demonstrating the first-order nature of the loss of **7a** at 24°C, measured as described for **5a** in Fig. 1.

$$\text{Cp}_2^*\text{M}\diagdown\text{H} \quad\longrightarrow\quad \text{Cp}_2^*\text{M}\diagdown\text{H} \qquad\qquad (28)$$

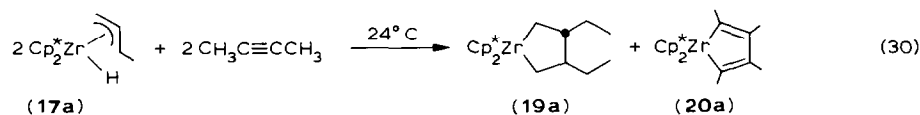(M = Zr, **7a**,   (M = Zr, **17a**;
M = Hf, **7b**)   M = Hf, **17b**)

ment requires weeks and results in three side products. At 80°C, the rearrangement is faster and cleaner, requiring 5 h and resulting in only one observed side product. These side products have not been definitively assigned, but hafnacyclopentanes are indicated by their ^{1}H NMR patterns.

The bisinsertion products $\text{Cp}_2^*\text{M}(C(CH_3)=CH(CH_3))_2$ have not been observed. However, a second equivalent of 2-butyne does react with the monoinsertion product **7a** to form zirconacyclopentene **18** (eq. 29), which can be isolated as a stable

$$\text{Cp}_2^*\text{Zr}\diagdown\text{H} \;+\; CH_3C\equiv CCH_3 \;\xrightarrow{24\,°C}\; \text{Cp}_2^*\text{Zr} \qquad\qquad (29)$$
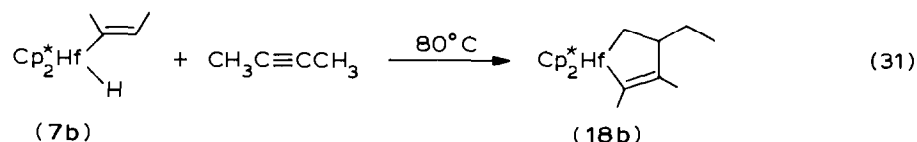
(**7a**)   (**18a**)

yellow microcrystalline solid. Qualitatively, reactions 28 and 29 proceed at the same rate, suggesting a common intermediate derived from **7a**. Surprisingly, zirconacyclopentene **18a** is not formed in the reaction of the crotyl-hydride species **17a** with 2-butyne. Rather, a 1 : 1 mixture of zirconacyclopentane **19a** and zirconacyclopentadiene **20a**, identified by comparison with the spectra of actual samples [18], is obtained (eq. 30). Zirconacyclopentene **18a** does not disproportionate to **19a** and

$$2\,\text{Cp}_2^*\text{Zr}\diagdown\text{H} \;+\; 2\,CH_3C\equiv CCH_3 \;\xrightarrow{24°C}\; \text{Cp}_2^*\text{Zr} \;+\; \text{Cp}_2^*\text{Zr} \qquad (30)$$

(**17a**)   (**19a**)   (**20a**)

20a, even after months at room temperature. Thus there appear to be two reaction manifolds. This is supported by the different reactivities of **7a** and **17a** with propyne and diphenylacetylene. While the products of these reactions have not been unambiguously identified, the reactions of **7a** with each of the alkynes and of **17a** with each of the alkynes produce distinctly different products.

$\text{Cp}_2^*\text{Hf(H)(C(Me)=CHMe)}$ (**7b**) also reacts with 2-butyne, forming the hafnium zirconacyclopentene **18b** (eq. 31) in 5 h at 80°C. As before, this reaction is less clean than the zirconium system, producing more free 1-butene, 10% hafnacyclo-

$$\text{Cp}_2^*\text{Hf}\diagdown\text{H} \;+\; CH_3C\equiv CCH_3 \;\xrightarrow{80°C}\; \text{Cp}_2^*\text{Hf} \qquad\qquad (31)$$

(**7b**)   (**18b**)

pentadiene **20b**, and 5% crotyl-hydride **17b**. The reaction of **17b** with 2-butyne has not been explored since **17b** has not yet been cleanly isolated.

The synthesis, characterization, and reactivity of bis(alkynyl) derivatives of permethyl-zirconocene and permethylhafnocene

The bis(propynyl) derivatives of permethylzirconocene and permethylhafnocene are prepared by treating $Cp_2^*MCl_2$ with two equivalents of propynyllithium (eq. 32)

$$Cp_2^*MCl_2 \ + \ 2\,LiC\equiv CCH_3 \ \longrightarrow \ Cp_2^*M(C\equiv CCH_3)_2 \ + \ LiCl \qquad (32)$$

$$(M = Zr, \ Hf)$$

$$(M = Zr, \ \mathbf{21a},$$
$$M = Hf, \ \mathbf{21b})$$
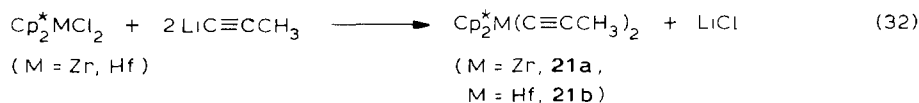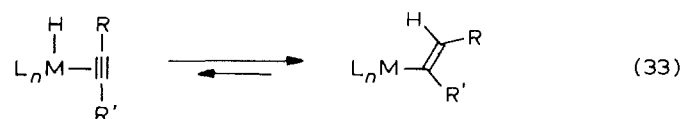
in dimethoxyethane. $Cp_2^*Zr(C\equiv CCH_3)_2$ (**21a**) was isolated as a pale yellow solid in 50% yield. $Cp_2^*Hf(C\equiv CCH_3)_2$ (**21b**) was isolated as a colorless solid in 70% yield. Both have been characterized by ^{13}C and ^1H NMR and IR spectroscopies (Table 1) and microanalyses. The NMR data are analogous to those found for the propynyl ligand of $Cp_2^*Zr(C\equiv CCH_3)(CH=CHCH_3)$ (**11**) [23]. Their IR spectra are diagnostic for disubstituted acetylenes [7] ($\nu(C\equiv C)$ 2090 and 2102 cm^{-1} for **21a** and **21b**, respectively).

Compounds **21a** and **21b** are remarkably stable, being unreactive with CO, H_2, and HPPh$_2$ [28]. Solutions of **21a** darken slowly, but no significant change is noted by ^1H NMR spectroscopy.

Discussion

Whereas the rapid insertion of alkyne into the M–H bonds of $Cp_2^*MH_2$ (M = Zr, Hf) is not surprising in light of previous findings [4,5], the subsequent rearrangements of the bis(alkenyl) products were unexpected. The results described above lead to the following postulates concerning the mechanism of these reactions, of which the reactivity of **1a** with propyne is representative (Scheme 1): (i) the insertion of two equivalents of propyne to afford the bis(propenyl) derivative **5a** is rapid, (ii) the β-hydrogen elimination from an sp^2-carbon in **5a** to afford the propyne adduct of the propenyl hydride complex occurs, (iii) reductive elimination of propene follows, (iv) the free propene coordinates to the propyne adduct **10** in orientations conducive to closure to either the kinetic or thermodynamic zirconacyclopentene **8** or **9**, and (v) the ring opening of **8** followed by loss of propene and recoordination of the propene to **10** in the proper orientation for closure to zirconacyclopentene **9** completes the sequence.

The β-hydrogen elimination from the sp^2-carbon proposed in Scheme 1 is the microscopic reverse of the propyne insertion, but it is not generally recognized as a kinetically accessible reaction; only one report has appeared in the literature [11,29]. The paucity of examples of β-hydrogen elimination from metal alkenyls as compared with the very common β-hydrogen elimination from metal alkyls is probably primarily attributable to the much higher reactivity of the C≡C bond relative to C=C bond rather than to any large difference in metal carbon σ-bond strengths. Indeed, the equilibrium (eq. 33) must lie far to the right for these Group IV alkenyl

$$L_nM-\overset{\overset{\displaystyle H \quad R}{|\ \ \ |}}{\underset{\underset{\displaystyle R'}{|}}{|||}} \quad \overset{\longrightarrow}{\longleftarrow} \quad L_nM-\overset{\displaystyle H}{\underset{\displaystyle R'}{\diagup\!\!\diagdown}}\!\!R \qquad (33)$$

derivatives, since no alkyne hydride species could be detected in solution for any of the alkenyl derivatives. This is also true in the equilibrium between the olefin-acetylene adducts and the zirconacyclopentenes (eq. 34), as evidenced by the

$$L_nM \rightleftharpoons L_nM \qquad (34)$$
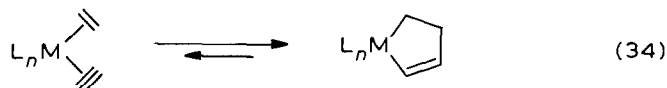
reactivity of these compounds with H_2 to produce only C_6 alkanes. Bis(pentamethylcyclopentadienyl)zirconacyclopentane, in contrast, yields both C_2 and C_4 alkanes.

In the case of the bis(alkenyl)zirconium derivatives, the irreversible reductive elimination of alkene that follows β-hydrogen elimination provides the modus operandi for their rearrangements. Whereas the magnitudes of the deuterium isotope effects for **5a**-$(\beta d)_2$ (4.9(5)) and **5a**-$(\alpha d)_2$ (1.03(10)) could be taken as evidence of a rate-limiting β-hydrogen elimination, the initial rapid generation of **5a** from $[Cp_2^* Zr(H)(CH{=}CHMe)(HC{\equiv}CMe)]$ suggests a pre-equilibrium regime with slow reductive elimination of propene. Hence, the deuterium isotope effect for **5a**-$(\beta d)_2$ is likely to be a composite of a thermodynamic effect of the pre-equilibrium and a primary kinetic effect of the slow reductive elimination. The stability of the hafnium derivative **5b** to these same rearrangements is probably due less to sluggish β-hydrogen elimination than to its reluctance to undergo reductive elimination to afford a Hf^{II} species [30].

Incorporation of propene-d_6 into zirconacyclopentene **8** when the rearrangement of **5a** is carried out in its presence suggests that propene is lost entirely from the coordination sphere of zirconium following the reductive elimination. The alternative, wherein propene remains coordinated to zirconium during reductive elimination, would appear to involve considerable strain. Similarly, the release of 50% of the available propene-d_0 from zirconacyclopentene **8** before 10% of **8** has been thermolyzed indicates that propene can also be lost from the coordination sphere of zirconium following ring opening (vide infra). The existence of other stable 16-electron alkyne adducts of permethylzirconocene [22] further supports the intermediacy of the Zr^{II}-alkyne adduct **10**.

The mechanism of propene coordination to **10** and ring closure is similar to that described for the formation of zirconaindans [20a,b] and zirconacyclopentadienes [20c], for which a stereospecific, concerted pathway is indicated. The positional preferences of the substituents in the five-membered ring are then determined by the coordination geometry, not by the π^* polarization rule set forth by Stockis and Hoffman [20e]. The difference in activation energies (1.2 kcal mol^{-1}) for closure to zirconacyclopentenes **8** and **9** favors **8** as the kinetic product. The sterically less demanding 3,4-dimethyl-substituted ring **9** is clearly favored thermodynamically, however, as evidenced by its lack of exchange with propene-d_6 (1 day, 80°C) and unusual reactivity with propyne.

The evidence for propene catalysis of the isomerization of **8** to **9** (eq. 35) contrasts

$$Cp_2^*Zr \underset{-\,=/}{\overset{+\,=/}{\rightleftharpoons}} \left[Cp_2^*Zr{-}||| \right] \xrightarrow{-\,=/} Cp_2^*Zr \qquad (35)$$
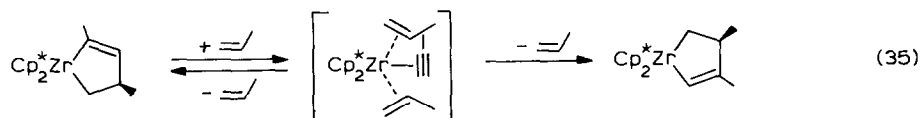
with the effect of added olefin in the rearrangement of zirconaindans [20c]. In those cases, no isomerization is observed; the sterically and, presumably, thermodynamically preferred isomer is the only one obtained. Moreover, exchange of free olefin into the zirconaindan is found to be independent of both the structure and concentration of the added olefin. Only initial rates were measured in this system, but it is possible that the large size of the benzene ring in the zirconaindans and of the added olefins prevent a mechanism in which excess alkene assists in the exchange of free alkene for coordinated alkene (the forward reaction shown in eq. 35).

Although the 2-butenyl-hydride complexes **7a** and **7b** have been studied in less detail, two plausible pathways may be envisioned for their rearrangement to the crotyl-hydride species **17a** and **17b**. The first, and perhaps most obvious, is β-hydrogen elimination from the sp^3(methyl) carbon followed by insertion of methylallene into a metal–hydride bond (eq. 36). This reactivity has been noted for 2-butenyl


$$(36)$$

(M = Zr, **7a**,
  M = Hf, **7b**)

(M = Zr, **17a**;
  M = Hf, **17b**)
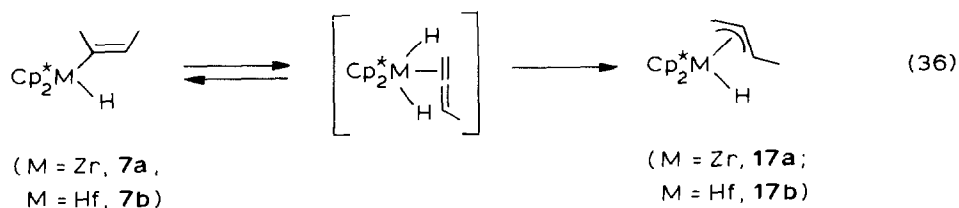
derivatives of iridium [11] and molybdenum [32] and is further supported by reaction of **1a** with allene to form $Cp_2^* Zr(H)(\eta^3\text{-}C_3H_5)$ [31].

The alternate pathway available to these systems is a mechanism involving initial reductive elimination of 2-butene followed by recoordination and tautomerization to **17a** and **17b** (eq. 37). This pathway is supported by previous observations that

$$(37)$$

(M = Zr, **7a**;
  M = Hf, **7b**)

(M = Zr, **17a**;
  M = Hf, **17b**)
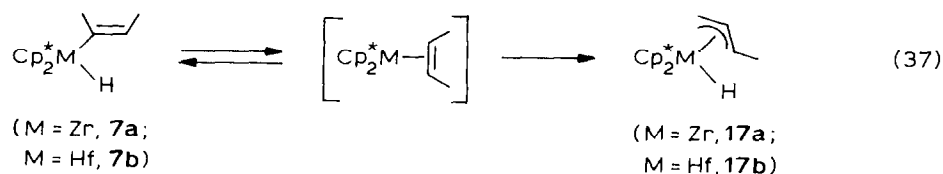
1-butene and *cis*- or *trans*-2-butene react with $\{Cp_2^* ZrN_2\}_2 N_2$ [18,31] to afford the *syn*-crotyl-hydride species **17a** (eq. 38). We favor the former mechanism, nonetheless,

$$(38)$$
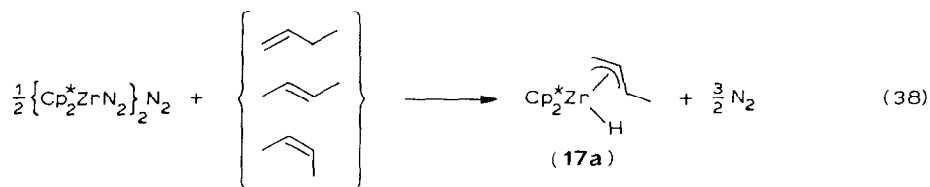
since we have shown these alkenyl hydride complexes are quite reluctant to undergo reductive elimination unless induced to do so by added alkyne (Scheme 1 and ref. 10).

The zirconium-crotyl-hydride species **17a** is known to react with one equivalent of 1- or 2-butene upon heating to yield zirconacyclopentane **19a** (eq. 39) [18,31]. That

$$\text{Cp}_2^*\text{Zr} \overset{\displaystyle\diagdown}{\underset{H}{\diagup}} \;\;\rightleftharpoons\;\; \left[\text{Cp}_2^*\text{Zr}{-}\|\right] + \left\{ \begin{array}{c} \\ \\ \\ \end{array} \right\} \;\;\overset{\Delta}{\longrightarrow}\;\; \text{Cp}_2^*\text{Zr}\langle\;\;\rangle \qquad (39)$$

(17a)   (19a)
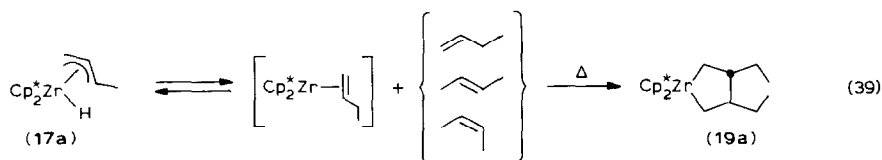
the reaction of **17a** with 2-butyne at room temperature results in formation of one-half equivalent of **19a** and one-half equivalent of zirconacyclopentadiene **20a** while the reaction of **7a** with 2-butyne at room temperature produces zirconacyclopentene **18a** is puzzling, particularly since **7a** isomerizes to **17a** under these conditions and the tautomerizations of allyl ligands are known to be facile in these zirconium systems [31]. Thus, neither **17a** nor a tautomer of **17a** can be an intermediate in the reaction of **7a** with 2-butyne. The mechanistic implications of these results are not currently understood.

As noted earlier, the spectroscopic data for the 2-butenyl hydride complexes **7a** and the major isomer of **7b** are unusual by comparison with the alkenyl derivatives with hydrogen at the α-carbon. The presence of the minor isomer of **7b** with NMR data similar to those of the alkenyl derivatives with hydrogen at the α-carbon suggests that there are two orientations for the alkenyl ligands in the equatorial plane of the $[\text{Cp}_2^*\text{M}]$ moiety (**A** vs. **B**) and that the more sterically demanding 2-butenyl ligand preferentially exists in a different orientation than the alkenyl

(A)   (B)
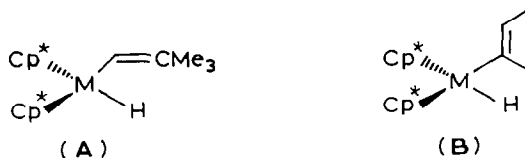
derivatives with hydrogen at the α-carbon. An equilibrium mixture of both forms ($\sim 1:1$) has been noted for a similar compound, $\text{Cp}_2^*\text{Nb(CO)(C(CH}_3)\!\!=\!\!\text{CHCH}_3)$ [33]. While Nuclear Overhauser Effect (NOE) difference spectroscopy on the major and minor isomers of **7b** failed to reveal which isomer had its vinylic hydrogen closer to its hydride, the irradiation of the hydride signal of **2b** produced a stronger NOE for the β-carbon's hydrogen, suggesting **A** as the preferred orientation of the alkenyl ligand in this compound and, by inference, **B** as the preferred orientation of **7a** and **7b**.

The reduced carbon–hydrogen coupling constants for the β-carbons of **7a** and the major isomer of **7b** indicate a decrease in the s-orbital character at these carbons and may indicate agostic [34] M $\cdots$ H–C interactions. The requisite vacant orbital exists in these coordinatively unsaturated 16-electron complexes (**C**), and the ^{1}H and ^{13}C

(C)
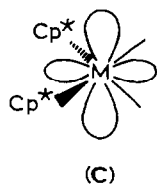
NMR signals of the β-hydrogens and -carbons of **7a** and of the major isomer of **7b** are shifted upfield, as expected from the alkyl cases documented thus far [34a]. In contrast, the ^{13}C NMR spectrum for the analogous niobium compound $Cp_2^* Nb$-$(CO)(C(CH_3)=CHCH_3)$, which is d^2 and has no vacant orbital, exhibits resonances at δ 136.0 and 128.8 ppm with carbon–hydrogen couplings of 156 and 150 Hz, respectively for the β-carbons of the two isomers [33b]. However, reduced C–H stretching frequencies in the IR spectra of **7a** and **7b** and significant changes in the isomer ratio upon deuteration of the β-carbon position of **7b**, which are also expected, are not observed. Thus the data could suggest the presence of the agostic interaction of a non-alkylidene [34b] sp^2-hybridized C–H bond, and would be the first such observation, but are not conclusive.

Conclusion

The most significant result of this study is the demonstration of reversible insertion of acetylenes into Group IV transition metal hydride bonds. Indeed, equilibrium 33 may be a general feature of transition metal alkenyls with a β-H that is evidenced only when there is an accessible decomposition pathway from the alkyne-hydride. The bis(alkenyl) derivatives of $[Cp_2^* Zr^{IV}]$ offer this feature. Morever the clean, kinetically well separated nature of their rearrangements has allowed some of the essential mechanistic details to be elucidated.

Experimental

General considerations

All manipulations were performed using glovebox or high vacuum line techniques. Solvents were dried over $LiAlH_4$ and stored over "titanocene" [35]. NMR solvents, benzene-d_6 and toluene-d_8, were dried over activated molecular sieves (4 A, Linde) and stored over "titanocene". Argon, nitrogen, hydrogen, and deuterium gases were passed over MnO on vermiculite and activated molecular sieves [36].

Propyne, 1-butyne, and propene were purified by several freeze-pump-thaw cycles at $-196°C$, then vacuum transferred at $24°C$. 2-Butyne and t-butylacetylene were transferred from activated molecular sieves. Propene-d_6 (Stohler) and 2-butyne-d_6 (MSD Isotopes) were used as received. Carbon monoxide (Matheson) and ^{13}CO (MRC-Mound) were used directly from the cylinders. $Cp_2^* ZrH_2$ (**1a**) [9c], $Cp_2^* HfH_2$ (**1b**) [12], $Cp_2^* M(H)(CH=CHCMe_3)$ (M = Zr (**2a**), Hf (**2b**)) [10], and $Cp_2^* M(H)(CH=CHPh)$ (M = Zr (**3a**), Hf (**3b**)) and $Cp_2^* M(CH=CHPh)_2$ (M = Zr (**4a**), Hf (**4b**)) [10] were prepared as previously described.

Many reactions were surveyed utilizing NMR spectroscopy. Any experiment described herein but not explicitly listed below was carried out in a sealed NMR tube utilizing ~ 30 mg of the starting material in ~ 0.3 ml of benzene-d_6 containing TMS, to which a known amount of an appropriate reagent was added before the tube was sealed at $-196°C$.

Nuclear magnetic resonance spectra were recorded on Varian EM 390 (90 MHz, ^1H), JEOL FX 90Q (89.56 MHz, ^1H; 22.50 MHz, ^{13}C; 13.70 MHz, ^2H) and Bruker WM 500 (500.13 MHz, ^1H; 125.8 MHz, ^{13}C; 76.5 MHz, ^2H) spectrometers and are reported in Table 1. ^1H Nuclear Overhauser Effect difference experiments were performed on the Bruker WM 500 using the NOEDIFF pulse program. Infrared spectra were recorded on a Beckman 4240 spectrophotometer and are reported in

cm^{-1}. Elemental analyses were determined by Dornis and Kolbe Microanalytical Laboratory, Galbraith Laboratories, Inc., and the Caltech Analytical Facility.

Procedures

(1) $Cp_2^*Zr(CH=CHCH_3)_2$ (5a). $Cp_2^*ZrH_2$ (1a) (1.82 g, 5.0 mmol) was placed in a round bottom flask with petroleum ether (8 ml). Propyne (18.0 mmol) was condensed onto the frozen solvent at $-196°C$. The blue (due to a dilute impurity in 1a) slurry was warmed to $-78°C$ and stirred for 60 min, becoming paler with time. Undissolved free propyne was removed under vacuum at $-78°C$. A cold filtration, without any warming above $-78°C$, yielded the off-white microcrystalline solid 5a (1.49 g, 66% yield). The air-sensitive solid was refrigerated under N_2. IR (Nujol, cm^{-1}): 1582w, 1570m, 1490w, 1306w, 1062w, 1023m, 994m, 974w. A microanalysis was not obtained because the compound's thermal instability in solution prevented adequate recrystallization [37].

(2) $Cp_2^*Zr(CD=CHCH_3)_2$ (5a-(αd)₂). Procedure 1 was followed using $Cp_2^*ZrH_2$ (0.41 g, 1.1 mmol) and $DC\equiv CCH_3$ (4.8 mmol) (Procedure 3), resulting in isolation of a light tan solid 5a-(αd)₂ (0.09 g, 18% yield). The low yield is due to the high solubility of these compounds in hydrocarbon solvents and the relatively large amount of solvent (8 ml)/amount of 1a used in this experiment. The solid was characterized by NMR only.

(3) $DC\equiv CCH_3$. D_2O was heated throughout the glass vacuum line and Toepler pump system in order to replace H^+ by D^+ at the glass sites. $LiC\equiv CCH_3$ (Aldrich, 1.36 g, 29.6 mmol) was placed in a round bottom flask. D_2O, which had been degassed by three freeze-pump-thaw cycles, was condensed in at $-78°C$. The ice was allowed to melt with stirring and the monodeuterated propyne was collected in the Toepler system until no more gas was evolved (~ 5 h). The propyne was determined to be 90% $DC\equiv CCH_3$ by reaction with $Cp_2^*ZrH_2$ (1a) and comparison of integrated intensities for the two vinyl positions.

(4) $Cp_2^*Zr(CH=CDCH_3)_2$ (5a-(βd)₂). Procedure 1 was followed using $Cp_2^*ZrD_2$ (generated in situ, Procedure 5), an excess of $HC\equiv CCH_3$, and 4 ml petroleum ether, resulting in isolation of the pale yellow solid 5a-(βd)₂ (0.46 g, 54% yield). The solid was characterized by NMR only.

(5) $Cp_2^*ZrD_2$ (1a-d_2). $\{Cp_2^*ZrN_2\}_2N_2$ [9] was placed in a round bottom flask with petroleum ether (25 ml). D_2 was admitted to the purple solution at 0°C, affording a blue solution after stirring for 1.5 h at 0°C. The D_2 atmosphere was removed under reduced pressure. A room temperature filtration removed a small amount of a yellow impurity from the blue solution. The solvent volume was reduced and the solution was used for Procedure 4. Compound 1a-d_2 was determined to be 90% $Cp_2^*ZrD_2$ by comparison of the integrated intensities of the two vinyl positions in 5a-(βd)₂.

(6) $Cp_2^*Hf(CH=CHCH_3)_2$ (5b). $Cp_2^*HfH_2$ (1b) (0.90 g, 2.0 mmol) was placed in a glass bomb with petroleum ether (20 ml). Propyne (13.2 mmol) was condensed into the bomb at $-196°C$. The colorless solution was warmed to room temperature and stirred overnight. The solution was transferred to a round bottom flask on a frit assembly. A room temperature filtration removed a pale yellow solid impurity. The solvent volume was reduced and the white solid 5b collected by cold filtration (3 crops, total yield 0.65 g, 60%). ^1H NMR shows a 10% impurity that repeated recrystallization did not remove [17] IR (Nujol, cm^{-1}): 2100w, 1571m, 1486m,

1152w, 1022m, 993m. Anal. Found: C, 57.96; H, 7.48. $C_{26}H_{40}Hf$ calcd.: C, 58.80; H, 7.59%.

(7) $Cp_2^* Zr(CH=CHCH_2CH_3)_2$ (6). $Cp_2^* ZrH_2$ (**1a**) (0.512 g, 1.4 mmol) was placed in a round bottom flask with petroleum ether (4 ml). 1-Butyne (5.6 mmol) was condensed into solution at −78°C and the solution was stirred at −78°C for 1 h, becoming yellow green. Since no solid was evident, the excess 1-butyne and solvent were removed under vacuum to yield the pale yellow-green oily solid **6** (isolated yield after scraping from flask, 0.30 g). Compound **6** was identified by ^1H NMR by analogy with **5a** and, because the work-up required the solution to warm above −78°C, was observed to be contaminated by the zirconacyclopentenes **12** and **13** as well as some $Cp_2^* Zr(CH=CHCH_2CH_3)(C≡CCH_2CH_3)$.

(8) $Cp_2^* Zr(H)(C(CH_3)=CHCH_3)$ (7a). $Cp_2^* ZrH_2$ (**1a**) 0.57 g, 1.6 mmol was placed in a round bottom flask with petroleum ether (5 ml). Excess 2-butyne was condensed into the blue solution at −78°C. The slurry became pink, then yellow when warmed just to the point that all the 2-butyne melted. The solution was immediately cooled to −78°C again. A cold filtration with no further warming yielded the pale yellow solid **7a** (0.26 g, 40% yield). The air-sensitive solid was refrigerated under N_2. IR (Nujol, cm^{-1}): 2724w, 2528w, 2040w, 1565sh, 1513m, 1490m, 1183w, 1164w, 1124w, 1106w, 1063w, 1025s, 870w, 803m, 792m, 724m, 606m, 591m, 512w, 449m. A microanalysis was not obtained because the compound's thermal instability in solution and the solid state prevented adequate recrystallization.

(9) $Cp_2^* Hf(H)(C(CH_3)=CHCH_3)$ (7b). $Cp_2^* HfH_2$ (**1b**) (0.605 g, 1.3 mmol) was placed in a round bottom flask on a frit assembly. Petroleum ether (20 ml) was condensed onto the white solid at −78°C. 2-Butyne (2.1 mmol) was condensed into solution at −78°C. The solution was allowed to warm to room temperature with stirring for 1.5 h. The pale yellow solution was filtered from a fine white solid (LiCl from the $Cp_2^* HfH_2$ synthesis). After reducing the filtrate volume and cooling the solution to −78°C did not produce a solid product, all the volatiles were removed, leaving the pale yellow solid **7b** (0.546 g, 81%). The solid was too soluble to be recrystallized. It was refrigerated under N_2. By NMR (Table 1), two isomers exist in a 90/10 ratio. IR (Nujol, cm^{-1}): 2718w, 1568s, br, 1486m, 1430m, 1021m, 875w, 802m. Anal. Found: C, 57.92; H, 7.62. $C_{26}H_{38}Hf$ calcd.: C, 57.08; H, 7.58%.

(10) $Cp_2^* Hf(D)(C(CH_3)=CDCH_3)$ (7b-d_2). Procedure 9 was followed using $Cp_2^* HfD_2$ (**1b**-d_2) (Procedure 11, 0.305 g, 0.7 mmol) and 2-butyne (1.1 mmol). The off-white solid **7b**-d_2 was isolated (0.267 g, 76%). ^1H NMR showed the absence of peaks due to the hydride and vinylic hydrogens, which were located in the ^2H NMR spectrum. There was no significant difference in the ratio of major to minor isomers (88/12). IR (Nujol, cm^{-1}): 2718w, 1560w, br, 1486sh, 1150sh, 1123m, br, 1021m, 795w.

(11) $Cp_2^* HfD_2$ (1b-d_2). $Cp_2^* HfH_2$ (**1b**) (0.485 g, 1.1 mmol) was placed in a round bottom flask on a frit assembly. Petroleum ether (∼ 15 ml) was condensed onto the white solid at −78°C. Deuterium gas (1 atm) was admitted and the solution was stirred at room temperature ∼ 2 h. The clear solution was then cooled to −78°C, the system was evacuated, and fresh deuterium gas admitted. This procedure was repeated four more times. The solution volume was then reduced (5 ml) and the off-white solid **1b**-d_2 collected by cold filtration (0.327 g, 67%). Residual hydrogen in the hydride position was < 3% by NMR.

(12) Cp$_2^*$Hf(H)(C(CD$_3$)=CHCD$_3$) (7b-d$_6$). Procedure 9 was followed using Cp$_2^*$HfH$_2$ (1b) (0.212 g, 0.5 mmol) and 2-butyne-d$_6$ (0.8 mmol). The pale yellow solid 7b-d$_6$ was isolated (0.105 g, 42%). ^{1}H, ^{2}H and ^{13}C NMR spectra were recorded to make definitive assignments for 7b.

(13) Cp$_2^*$ZrCH$_2$CH(CH$_3$)CH=C(CH$_3$) (8). Cp$_2^*$Zr(CH=CH(CH$_3$))$_2$ (5a) (1.46 g, 3.3 mmol) was placed in a round bottom flask with petroleum ether (8 ml). The solution was stirred three days, becoming bright yellow. After a room temperature filtration removed a small amount of a fine solid [37], the solvent volume was reduced (4 ml) and the bright yellow microcrystalline solid was collected by cold filtration (3 crops, total yield 1.09 g, 75%). The solid was pure 8 by NMR, with no evidence of 9. IR (Nujol, cm^{-1}): 2793m, 1554w, 1490w, 1355w, 1299w, 1285w, 1166w, 1113w, 1022m, 833m, 805w. Anal. Found: C, 70.23; H, 9.31. C$_{26}$H$_{40}$Zr calcd.: C, 70.36; H, 9.08%.

(14) Cp$_2^*$ZrCH$_2$CH(CH$_3$)$_3$C(CH$_3$)=CH (9). Zirconacyclopentene 8 (0.80 g, 1.8 mmol) was placed in a small glass bomb with toluene (5 ml). Excess propene was condensed in at −78°C. The yellow solution was heated to 80°C with stirring for 22 h. The solution was transferred to a round bottom flask on a frit assembly. The volatiles were removed under reduced pressure and petroleum ether (5 ml) was condensed in at −78°C. The yellow-orange solution was filtered at room temperature, leaving a small amount of a tan solid impurity. The solvent volume was reduced (2 ml) and the bright yellow microcrystalline solid 9 was collected by cold filtration (2 crops, total yield 0.57 g, 71%). IR (C$_6$H$_6$): 2944s, 2898s, 2856sh, 1555m, 1450sh, 1379m, 1356m, 1278w, 1064w, 1013w, 809w, 725w. Anal. Found: C, 70.28; H, 9.13. C$_{26}$H$_{40}$Zr calcd.: C, 70.36; H, 9.08%.

(15) Cp$_2^*$Zr(H)(η^3-CH$_2$CHCHCH$_3$) (17). Cp$_2^*$ZrH$_2$ (1a) (1.31 g, 3.1 mmol) was placed in a round bottom flask with petroleum ether (10 ml). Excess 2-butyne was condensed into the blue solution at −23°C, which rapidly changed to yellow. After ~ 1 h the volatiles were removed and fresh petroleum ether was condensed onto the yellow solid [39]. The solution was stirred at room temperature for one week. The solvent volume was reduced (3 ml). An oily yellow-brown solid was isolated by cold filtration. Recrystallization from fresh petroleum ether yielded the pale yellow solid 17 (0.45 g, 34%) with NMR spectra identical to those obtained previously [38].

(16) Cp$_2^*$ZrCH$_2$CH(CH$_2$CH$_3$)C(CH$_3$)=C(CH$_3$) (18). Cp$_2^*$Zr(H)(C(CH$_3$)=CH(CH$_3$)) (7a) (0.82 g, 2.0 mmol) was placed in a small glass bomb with toluene (5 ml). 2-Butyne (2.5 mmol) was condensed in at −196°C. The solution was warmed to room temperature and stirred four days. The orange solution was transferred to a round bottom flask on a frit assembly. The volatiles were removed under reduced pressure and petroleum ether (5 ml) was condensed in at −78°C. The solution was filtered at room temperature, leaving a small amount of pale yellow solid. The solvent volume was reduced (2 ml) and the bright yellow microcrystalline solid 18 was collected by cold filtration (2 crops, total yield 0.62 g, 67%). IR (Nujol, cm^{-1}): 1554m, 1490sh, 1365sh, 1159w, 1060w, 1021m, 921w, 928w, 706w, Anal. Found: C, 71.14; H, 9.05. C$_{28}$H$_{44}$Zr calcd.: C, 71.27; H, 9.40%.

(17) Cp$_2^*$Zr(C≡CCH$_3$)$_2$ (21a). Cp$_2^*$ZrCl$_2$ [9] (1.17 g, 2.7 mmol) and Li(C≡CCH$_3$) (Aldrich, 0.38 g, 8.3 mmol) were placed in a round bottom flask. Dimethoxyethane (DME) (20 ml) was condensed in and the solution was warmed to room temperature with stirring. After 4.5 h, the volatiles were removed and petroleum ether (15 ml)

was condensed in. The LiCl was filtered away. The solvent volume was then reduced and the pale yellow solid **21a** was isolated (2 crops, 0.59 g, 50%). IR (Nujol, cm^{-1}): 2090m, 1062w, 1023m, 970m. Anal. Found: C, 70.81; H, 8.23. $C_{26}H_{36}Zr$ calcd.: C, 71.00; H, 8.25%.

(18) $Cp_2^*Hf(C\equiv CCH_3)_2$ (21b). $Cp_2^*HfCl_2$ [12] (0.83 g, 1.6 mmol) and Li(C≡CCH$_3$) (0.20 g, 4.3 mmol) were reacted as in Procedure 17, except the DME solution was refluxed. The white solid **21b** was isolated (2 crops, 0.59 g, 70%). IR (C_6D_6, cm^{-1}): 2988m, 2957m, 2909s, 2854m, 2723w, 2102s, 1489m, 1428m, 1379m, 1066w, 1027m, 976m. Anal. Found: C, 59.10; H, 6.71. $C_{26}H_{36}Hf$ calcd.: C, 59.25; H, 6.88%.

(19) $Cp_2^*Zr(CH=CHCH_3)(C\equiv CCH_3)$ (11). $Cp_2^*ZrH_2$ **(1a)** (1.32 g, 3.6 mmol) was placed in a round bottom flask with toluene (20 ml). A propyne atmosphere was maintained at 760 Torr until uptake ceased. The orange solution was heated overnight just below reflux. All volatiles were removed under vacuum and petroleum ether (10 ml) was condensed in. A cold filtration yielded the pale yellow solid **11** (0.52 g, 33%, not optimized) with spectra analogous to those previously observed [23].

(20) Reactions of 5a, 5a-($\beta d)_2$, 8 and 9 with excess propyne. These experiments were carried out on NMR samples and the products identified by comparison with the NMR spectra of actual samples, except for the product of the reaction of **9** with propyne, which was identified solely by analysis of its 500 MHz ^{1}H spectrum. A typical experiment involved: the compound (~ 30 mg) was placed in a sealable NMR tube with benzene-d_6 (~ 0.4 ml). Propyne (2–5 equiv.) was condensed in at −196°C and the tube was sealed. The tube was warmed to room temperature and its ^{1}H (and ^{2}H for **5a-($\beta d)_2$**) spectrum recorded.

(21) $Cp_2^*ZrCD(H)CD(CH_3)CH=C(CH_3)$ (8-d_2)$_A$ and $Cp_2^*ZrCH-(D)CH(CH_3)CD=C(CH_3)$ (8-d_2)$_B$. Zirconacyclopentenes **(8-d_2)$_A$** and **(8-d_2)$_B$** were formed in NMR tube reactions from **5a-($\beta d)_2$** and **5a-($\alpha d)_2$**, respectively and identified by ^{1}H and ^{2}H NMR. A typical experiment involved: compound **5a-(d)$_2$** (~ 30 mg) was placed in a sealable NMR tube with benzene-d_6 (~ 0.4 ml) and the tube was sealed at low temperature. The tube was brought to room temperature and allowed to react. The reaction kinetics could be observed for these systems (Procedure 28).

(22) Reactions of 5a, 8 and 9 in the presence of excess propene-d_6. These experiments were carried out on NMR samples and the products identified and quantified by ^{1}H and ^{2}H spectra. Kinetic measurements were made in similar experiments with perprotio propene (Procedure 29).

(23) Reactions of 5a and 5b with CO. Compounds **5a** and **5b** react with 2 equiv. of CO in NMR and bomb reactions to produce enediolates **14a** and **14b**, identified by ^{1}H and ^{13}C NMR and IR and by analogy to experiments with $Cp_2^*Zr(CH_3)_2$ [9]. A typical NMR experiment involved: compound **5** (~ 30 mg) was placed in a sealable NMR tube with benzene-d_6 (~ 0.4 ml). One atmosphere of CO was admitted at −78°C and the tube was then sealed at −196°C. Upon warming, the solution quickly became purple **(14a)** or red **(14b)**. The reactions are quantitative by NMR, with no evidence of $Cp_2^*M(CO)_2$. The stoichiometry of the reaction was checked by Toepler pump experiment: compound **5b** (0.14 g, 2.7×10^{-4} mol) was placed in a glass bomb with toluene (10 ml). CO (1.70×10^{-3} mol, 6.3 equiv.) was added to the frozen colorless solution. The solution was warmed to room temperature with stirring. After 3.5 h, the red solution was cooled to −78°C and the

remaining CO (1.29×10^{-3} mol) was collected by Toepler pump. Analysis indicated that 2.1 equiv. of CO were consumed per mole of Hf.

Attempts to isolate **14a** and **14b** have not yielded clean products, probably because insufficient CO pressure was used. An additional problem with the preparation of **14a** is the thermal instability of **5a**. IR (C_6D_6, cm^{-1}) **14a**: 3017m, 2981m, 2915s, 2854m, 2732w, 1636m, 1603w, 1561w, 1523m, 1440m, 1381m, 1313m, 1291s, 1268m, 1150w, 1092w, 1028w, 951s, 923m. IR (C_6D_6, cm^{-1}) **14b**: 3040w, 2978m, 2916s, 2858m, 2734w, 1631m, 1528m, 1495w, 1437m, 1381m, 1315m, 1292s, 1269m, 1092w, 1028m, 1009w, 950s, 921m, 757w.

(24) Reactions of 8 and 9 with CO. Zirconacyclopentenes **8** and **9** react with 1 equiv. of CO in NMR reactions to produce dienolates **15** and **16**, identified by ^{1}H and ^{13}C NMR and IR and by analogy to experiments with $Cp_2^\star ZrCH_2CH_2CH_2CH_2$ [9]. A typical NMR experiment involved: zirconacyclopentene (~ 30 mg) was placed in a sealable NMR tube with benzene-d_6 (~ 0.4 ml). CO was condensed in as described in Procedure 23. Upon warming the yellow solutions became orange-brown. The reactions are quantitative by NMR. The stoichiometry of the reaction was checked by Toepler pump experiment as described in Procedure 23: zirconacyclopentene **9** (0.13 g, 3.0×10^{-4} mol), toluene (5 ml), CO (2.6×10^{-3} mol, 8.7 equiv.), 1 h stirring, red solution resulted; CO collected (2.31×10^{-3} mol). Analysis indicated that 1.0 equiv. of CO were consumed per mol of Zr.

Dienolate **15** has been isolated as follows: zirconacyclopentene **8** (0.20 g, 0.45 mmol) was placed in a small glass bomb with petroleum ether (5 ml). Excess CO was admitted at $-78°C$. The yellow solution was warmed to room temperature and stirred 20 min. The resulting violet solution was transferred to a round bottom flask attached to a frit assembly and the solvent volume reduced (2 ml). The lavender solid **15** was isolated by cold filtration (0.09 g, 44%) and characterized by NMR and IR. Attempts to isolate dienolate **16** produced oils and have not been pursued. IR (C_6D_6, cm^{-1}) **15**: 2980m, 2911s, 2862m, 2760w, 2734w, 1942m, 1845m, 1638w, 1593m, 1579w, 1488m, 1446m, 1388n, 1347s, 1301w, 1243s, 1188m, 1141m, 1028m.

As described in Results, dienolates **15** and **16** rearrange, as observed by ^{1}H NMR. Compound **15** appears to form one new dienolate, but **16** rearranges to more than one product, whose NMR spectra are not readily interpreted.

(25) Reactions of 5a, 8 and 9 with H$_2$. All three compounds **5a**, **8** and **9** react with excess H$_2$ to produce $Cp_2^\star ZrH_2$ (**1a**) and alkane. A typical NMR reaction involved: compound **8** (~ 30 mg) was placed in a sealable NMR tube with benzene-d_6 (~ 0.4 ml). H$_2$ was admitted at $-196°C$ and the tube was sealed. The tube was warmed to room temperature and allowed to react. The reaction rate slowed as H$_2$ was consumed. The reactions were followed by ^{1}H NMR and the products identified by comparison with literature reports [9,40].

(26) $Cp_2^\star Zr(H)(\eta^3\text{-}CH_2CHCHCH_3)$ (17) and 2-butyne. Compound **17** (0.31 g, 7.4×10^{-5} mol) was placed in a sealable NMR tube with benzene-d_6. 2-Butyne (7.4×10^{-5} mol) was condensed in and the tube was sealed. After 1 day the reaction was complete; the products, $Cp_2^\star ZrCH_2CH(CH_2CH_3)CH(CH_2CH_3)CH_2$ (**19**) and $Cp_2^\star ZrC(CH_3)=C(CH_3)C(CH_3)=C(CH_3)$ (**20**), were identified by comparison with spectra of authentic samples [18].

(27) Kinetic measurements of the rearrangement of 5a. The rates of rearrangement were followed by monitoring the decrease in peak height [41] of the Cp* resonance

of **5a**, **5a**-$(\alpha d)_2$ or **5a**-$(\beta d)_2$ relative to an internal, nonreacting standard of TMS. Reactions proceeded at the ambient laboratory temperature, which was 24°C and was constant to ± 1°C over the day required for the experiments with **5a** and **5a**-$(\alpha d)_2$, and ± 2°C over the week required for **5a**-$(\beta d)_2$. EM-390 spectra were recorded at appropriate intervals.

A typical ^{1}H NMR experiment involved 30 mg of **5a** dissolved in 0.30 ml of benzene-d_6 containing TMS. The NMR tube was sealed with N$_2$ (< 1 atm). As the rearrangement progressed, the Cp* resonance of **5a** lost intensity, and plots of the decay of the ratio of the Cp* peak height/TMS peak height as a function of time showed first-order behavior for three half-lives.

The observed rate constants were derived from the slopes of the semilog plots (Fig. 1), yielding k_{obs}(**5a**) $2.12(21) \times 10^{-5}$ s^{-1} (correlation coefficient $r^2 = 1.00$), k_{obs}(**5a**-$(\alpha d)_2$) $2.05(21) \times 10^{-5}$ s^{-1} ($r^2 = 0.99$), and k_{obs}(**5a**-$(\beta d)_2$) $4.38(44) \times 10^{-6}$ s^{-1} ($r^2 = 0.99$) and isotope effects of $k_H/k_{\alpha D} = 1.03(10)$ and $k_H/k_{\beta D} = 4.85(48)$. Assuming the Eyring equation holds ($\kappa = 1$) [25], $\Delta G^{\ddagger}$(297 K) may be calculated: 23.7(2) kcal mol^{-1}.

The reactions were not run over a range of temperatures, so $\Delta H^{\ddagger}$ and $\Delta S^{\ddagger}$ can not be calculated. When **5a** was no longer evident, however, **8** and some **9** were observed by NMR. The Arrhenius equation [25] can thus be used to calculate ΔE_a 1.2 kcal mol^{-1}, assuming the difference in relative amounts of **8** and **9** is a kinetic effect, i.e. [**8**]/[**9**] $= k_8/k_9$.

The error given in parentheses above represents one standard deviation estimated from the repetition of some of the experiments. An analysis of residuals for each line always gave a smaller error value.

(28) Kinetic measurements of the rearrangement of 8. The rates of rearrangement were followed by monitoring the decrease in peak height [42] of the vinylic resonances of **8** and (**8**-d_2)$_A$ relative to an internal, nonreacting standard of the residual protons of benzene-d_6. Compound (**8**-d_2)$_B$ was not examined because the vinylic resonance was absent and no other peak in the ^{1}H NMR spectrum was sufficiently isolated to monitor. The NMR samples from Procedure 27 were utilized for these experiments. The NMR tubes were heated to 78 ± 1°C in an oil bath. EM-390 spectra were recorded at appropriate intervals by removing the tubes from the oil bath and quickly cooling them to room temperature (24°C), at which the rearrangements are negligibly slow.

The observed rate constants were derived from the slopes of the semilog plots (Fig. 2), yielding k_{obs}(**8**) $2.97(3) \times 10^{-5}$ s^{-1} ($r^2 = 0.99$) and k_{obs}((**8**-d_2)$_A$ $2.78(28) \times 10^{-5}$ s^{-1} ($r^2 = 0.99$) and a kinetic isotope effect of 1.07(10). Assuming large error bars (vide supra), this value is not significant but it is in the direction expected (see Results). Again assuming the Eyring equation holds ($\kappa = 1$), $\Delta G^{\ddagger}$(351 K) 27.9(13) kcal mol^{-1}.

(29) Kinetic measurements of the rearrangements of 5a and 8 in the presence of propene. Procedures analogous to those of Procedure 27 and 28 were used, except none of the labelled compounds was used. A typical ^{1}H NMR experiment involved ~ 30 mg of **5a** or **8**, weighed accurately and placed in a sealable NMR tube. Propene (~ 0, 2, or 10 equiv.) was expanded into a calibrated gas volume, then condensed into a calibrated liquid volume containing benzene-d_6 with TMS (~ 0.4 ml). The volume of this solution was measured at room temperature and the solution was then transferred to the NMR tube, which was subsequently sealed under N$_2$ (3 atm).

The EM-390 spectra were recorded at appropriate intervals as the reactions proceeded at ambient laboratory temperature, $28 \pm 1°C$, for **5a** and $79 \pm 1°C$ for **8**. The reactions were first order in **5a** for 3 half-lives and in **8** for 2 half-lives. The observed rate constants were derived from the slopes of the semilog plots (Fig. 3 for **5a**), yielding k_{obs}(0 equiv) $2.87(21) \times 10^{-5}$ s^{-1} ($r^2 = 0.99$), k_{obs}(2.1 equiv) $3.26(21) \times 10^{-5}$ s^{-1} ($r^2 = 1.00$), and k_{obs}(9.7 equiv) $2.94(21) \times 10^{-5}$ s^{-1} ($r^2 = 0.98$) for **5a** and k_{obs}(0 equiv) $5.9(6) \times 10^{-5}$ s^{-1} ($r^2 = 0.98$), k_{obs}(2.2 equiv) $6.7(7) \times 10^{-4}$ s^{-1} ($r^2 = 1.00$), and k_{obs}(8.3 equiv) $8.7(9) \times 10^{-5}$ s^{-1} ($r^2 = 0.99$) for **8**. Thus the rate-determining step in the rearrangement of **5a** is independent of propene concentration, but a plot of the rate of isomerization of **8** vs. the concentration of added propene yielded a straight line $k_{obs} = k + k'$[propene], with $k = 5.9(6) \times 10^{-5}$ s^{-1} and k' $2.1(2) \times 10^{-5}$ l mol^{-1} s^{-1} ($r^2 = 1.00$). The error bars represent one standard deviation determined from the three experiments for **5a**, and an estimated error of 10% for **8**. Analysis of residuals for each line always gave a smaller error value.

(30) Kinetic measurements of the rearrangement of 7a. Procedures analogous to those of Procedure 27 were used. Only one experiment was followed. $Cp_2^*ZrH_2$ (**1a**) (0.051 g, 1.40×10^{-4} mol) was placed in a sealable NMR tube with benzene-d_6 and TMS. 2-Butyne (1.40×10^{-4} mol) was condensed in and the tube was sealed. $Cp_2^*Zr(H)(C(CH_3)=CH(CH_3))$ (**7a**) was formed instantaneously. The rearrangement proceeded at the ambient laboratory temperature ($24 \pm 1°C$). EM-390 spectra were recorded at appropriate intervals. The observed first-order rate constant was determined from the slope of the semilog plot (Fig. 4), yielding k_{obs} $1.00(10) \times 10^{-5}$ s^{-1} ($r^2 = 0.99$). $\Delta G^{\ddagger}$(297 K) may be calculated by assuming the Eyring equation holds ($\kappa = 1$) [25]: 24.2(2) kcal mol^{-1}.

Acknowledgments

References

1 G.W. Parshall, Homogeneous Catalysis, Wiley, New York, N.Y., 1980.
2 (a) J.P. Collman and L.S. Hegedus, Principles and Applications of Organotransition Metal Chemistry, University Science Books, Mill Valley, California, 1980; (b) R.F. Heck, Organotransition Metal Chemistry: A Mechanistic Approach, Academic Press, San Francisco, CA, 1974.
3 For example see: (a) S. Otsuka and A. Nakamura, Adv. Organomet. Chem., 14 (1976) 245; (b) A. Nakamura and S. Otsuka, J. Am. Chem. Soc., 95 (1973) 7262; ibid., 94 (1972) 1886; (c) B. Longato and S. Bresadola, Inorg. Chem., 21 (1982) 168; (d) H.C. Clark and C.S. Wong, J. Am. Chem. Soc., 100 (1978) 7073; J. Organomet. Chem., 92 (1975) C31; (e) H.C. Clark and C.R. Milne, J. Organomet. Chem., 161 (1978) 51.
4 (a) J. Schwartz and J.A. Labinger, Angew. Chem. Int. Ed. Engl., 15 (1976) 333; (b) D.W. Hart, T.F. Blackburn, and J. Schwartz, J. Am. Chem. Soc., 97 (1975) 679; (c) J.A. Labinger, D.W. Hart, W.E. Seibert, and J. Schwartz, J. Am. Chem. Soc., 97 (1975) 3851.
5 D.E. Van Horn and E. Negishi, J. Am. Chem. Soc., 100 (1978) 2252.
6 P.C. Wailes, H. Weigold, and A.P. Bell, J. Organomet. Chem., 27 (1971) 373.
7 R. Jiminez, M.C. Barral, V. Moreno, and A. Santos, J. Organomet. Chem., 182 (1979) 353.

8 (a) P. Czisch and G. Erker, J. Organomet. Chem., 253 (1983) C9; (b) G. Erker, K. Kropp, J.L. Atwood, and W.E. Hunter, Organometallics, 2 (1983) 1555.

9 (a) J.M. Manriquez, D.R. McAlister, R.D. Sanner, and J.E. Bercaw, J. Am. Chem. Soc., 100 (1978) 2716; (b) P.T. Wolczanski and J.E. Bercaw, Acc. Chem. Res., 13 (1980) 121; (c) D.R. McAlister, D.K. Erwin, and J.E. Bercaw, J. Am. Chem. Soc., 100 (1978) 5966.

10 D.M. Roddick, Ph.D. Thesis, California Institute of Technology, 1984.

11 Only one other report of β-H elimination from an sp^2-carbon appears in the literature. J. Schwartz, D.W. Hart, and B. McGiffert, J. Am. Chem. Soc., 96 (1974) 5613.

12 D.M. Roddick, M.D. Fryzuk, P.F. Seidler, G.L. Hillhouse, and J.E. Bercaw, Organometallics, in press.

13 The characterization of **2b** is complete and has been reported [10]. Compound **2a** had been fully characterized. The isolated solid is 92% **2a** and 8% another, unidentified, compound (NMR) [14]

14 D.M. Roddick and J.E. Bercaw, unpublished results.

15 (a) S.A. Cohen, Ph.D. Thesis, California Institute of Technology, 1978; (b) S.J. McLain, C.D. Wood, and R.R. Schrock, J. Am. Chem Soc., 101 (1979) 4558; (c) B. Wrackmeyer, Spectros. Int. J., 1 (1982) 201.

16 (a) P.W. Jolly and R. Mynott, Adv. Organomet. Chem., 19 (1981) 257; (b) M.H. Chisolm and S. Godleski, Prog. Inorg. Chem., 20 (1976) 299; (c) G.C. Levy, R.L. Lichter, and G.L. Nelson, Carbon-13 Nuclear Magnetic Resonance Spectroscopy, 2nd ed., Wiley, New York, N.Y. 1980.

17 In both ^{13}C and ^{1}H NMR spectra, the only impurity peak observed is assignable to a pentamethyl-cyclopentadienyl ligand. Since the chemical analysis figures are good and a weak band appears at 2100 cm^{-1} in the IR, one might postulate $Cp_2^*Hf(H)(C\equiv CCH_3)$ as the impurity. A similar suggestion has been made in the formation of $Cp_2^*Hf(H)(CH=CHCMe_3)$ (**2b**) [14].

18 R.D. Sanner, Ph.D. Thesis, California Institute of Technology, 1977.

19 J.X. McDermott, M.E. Wilson, and G.M. Whitesides, J. Am. Chem. Soc., 98 (1976) 6529.

20 (a) G. Erker and K. Kropp, J. Am. Chem. Soc., 101 (1979) 3659; (b) K. Kropp and G. Erker, Organometallics, 1 (1982) 1246; (c) V. Skibbe and G. Erker, J. Organomet. Chem., 241 (1983) 15; (d) G. Erker, K. Engel, J.L. Atwood, and W.E. Hunter, Angew. Chem. Int. Ed. Engl., 22 (1983) 494; (e) A. Stockis and R. Hoffmann, J. Am. Chem. Soc., 102 (1980) 2952 and references cited therein.

21 The transition state energy difference was calculated using the Arrhenius equation (see Experimental).

22 R.S. Threlkel, Ph.D. Thesis, California Institute of Technology, 1980.

23 R.S. Threlkel, S.A. Cohen, and J.E. Bercaw, unpublished results.

24 Since the rates of reactions were measured only at one temperature, the activation barriers, $\Delta G^{\ddagger}$'s, were calculated using the Eyring equation. κ (transmission coefficient) was assumed to be unity [25].

25 (a) P.W. Atkins, Physical Chemistry, W.H. Freeman, San Francisco, 1978, Chapter 26; (b) C.G. Hill, Jr., An Introduction to Chemical Engineering Kinetics and Reactor Design, Wiley, New York, New York, 1977, Chapter 7.

26 T.H. Lowry and K.S. Richardson, Mechanism and Theory in Organic Chemistry, Harper and Row Publishers, San Francisco, CA, 1976, Chapter 2.

27 D.A. Straus and R.H. Grubbs, personal communication.

28 W.J. Evans and J.L. Atwood, Organometallics, 2 (1983) 709.

29 Another example has since appeared: $Cp_2^*Nb(CO)(C(CH_3)=CH(CH_3))$ loses CO to yield $Cp_2^*Nb(H)(C(CH_3)\equiv C(CH_3))$ [33].

30 It has also been observed that the Hf^{II} species $\{Cp_2^*HfN_2\}_2N_2$ is much more difficult to make than the zirconium analogue $\{Cp_2^*ZrN_2\}_2N_2$, the difficulty lying in the reduction of the starting $Cp_2^*HfCl_2$ [12].

31 (a) R.D. Sanner, D.K. Erwin, S.A. Cohen, C. Wood, L. Messerle, R.R. Schrock, and J.E. Bercaw, manuscript in preparation; (b) D.K. Erwin, Ph.D. Thesis, California Institute of Technology, 1979.

32 M. Bottrill and M. Green, J. Am. Chem. Soc., 99 (1977) 5795.

33 (a) N.M. Doherty, Ph.D. Thesis, California Institute of Technology, 1984; (b) C. McDade, N.M. Doherty, J.E. Bercaw, unpublished results.

34 (a) M. Brookhart and M.L.H. Green, J. Organomet. Chem., 250 (1983) 395; (b) R.R. Schrock, Acc. Chem. Res., 12 (1979) 98.

35 R.H. Marvich and H.H. Brintzinger, J. Am. Chem. Soc., 93 (1971) 2046.

36 T.L. Brown, D.W. Dickerhoff, D.A. Bofus, and G.L. Morgan, Rev. Sci. Instrum., 22 (1962) 491.

37 A small amount of insoluble material was always evident when **5a** was placed in benzene-d_6 or was used to synthesize the zirconacyclopentenes **8** and **9** (Procedures 13 and 14). For kinetics experiments with **5a**, this was centrifuged out of solution to the top of the sealed NMR tube. Compounds **8** and **9** could be isolated cleanly.

38 Compound **17a** can be formed more rapidly (<1 day) from $\{Cp_2^* ZrN_2\}_2 N_2$ and *trans*-2-butene. Its further characterization has been described [18].

39 If excess 2-butyne is left in the reaction mixture, zirconacyclopentene **18** will form as described in Procedure 16.

40 C.J. Pouchert and J.R. Campbell, The Aldrich Library of NMR Spectra, Vol. I, Aldrich Chemical Company, Inc., Milwaukee, Wisconsin, 1974.

41 The peak shape did not change during reaction, and accurate integrations were difficult to obtain due to the proximity of resonances not due to Cp* of the starting compound. Thus, peak heights were adjudged sufficiently accurate for this study.

42 The resonances due to the Cp* protons of **8** and **9** overlap; only the vinylic resonances were sufficiently separated. The peak shape did not change during reaction, so peak heights were adjudged sufficiently accurate for this study.